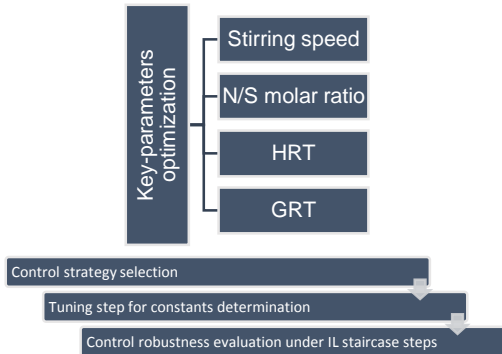
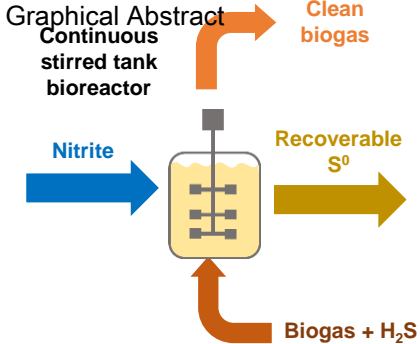


Journal of Hazardous Materials

Anoxic biogas biodesulfurization promoting elemental sulfur production in a Continuous Stirred Tank Bioreactor --Manuscript Draft--

Manuscript Number:	HAZMAT-D-20-05363R2
Article Type:	Research Paper
Keywords:	Biogas; elemental sulfur; CSTBR; Hydrogen sulfide; autotrophic denitrification
Corresponding Author:	Martín Ramírez, Ph.D. University of Cadiz Puerto Real, SPAIN
First Author:	José Joaquín González-Cortés, M.Sc
Order of Authors:	José Joaquín González-Cortés, M.Sc Sandra Torres-Herrera, M.Sc Fernando Almenglo, Ph.D Martín Ramírez, Ph.D. Domingo Cantero, Professor
Abstract:	<p>Biological desulfurization of biogas has been extensively studied using biotrickling filters (BTFs). However, the accumulation of elemental sulfur (S₀) on the packing material limits the use of this technology. To overcome this issue, the use of a continuous stirred tank bioreactor (CSTBR) under anoxic conditions for biogas desulfurization and S₀ production is proposed in the present study. The effect of the main parameters (stirring speed, N/S molar ratio, hydraulic residence time (HRT) and gas residence time (GRT)) on the bioreactor performance was studied. Under an inlet load (IL) of 100 g S-H₂S m⁻³ h⁻¹ and a GRT of 119 s, the CSTBR optimal operating conditions were 60 rpm, N/S molar ratio of 1.1 and a HRT of 42 h, in which a removal efficiency (RE) and S₀ production of 98.6 ± 0.4% and 88% were obtained, respectively. Under a GRT of 41s and an IL of 232 g S-H₂S m⁻³ h⁻¹ the maximum elimination capacity (EC) of 166.0 ± 7.2 g S-H₂S m⁻³ h⁻¹ (RE = 71.7 ± 3.1%) was obtained. A proportional-integral feedback control strategy was successfully applied to the bioreactor operated under a stepped variable IL.</p>



- Nitrite-reducing sulfide-oxidizing bacteria is sensitive to shear stress forces.
- N/S molar ratios below 1.1 mol mol^{-1} compromises the H_2S RE.
- The highest dilution times biomass product was found at an HRT of 42 h.
- An EC of $166.0 \pm 7.2 \text{ gS-H}_2\text{S m}^{-3} \text{ h}^{-1}$ (RE = 71.7%) was obtained under a GRT of 41s.
- Proportional – Integral control worked successfully under stepwise variable IL.

1 **Anoxic biogas biodesulfurization promoting elemental sulfur production in a**
2 **Continuous Stirred Tank Bioreactor**

3

4 *José Joaquín González-Cortés, Sandra Torres-Herrera, Fernando Almenglo, Martín*
5 *Ramírez*, Domingo Cantero*

6 Department of Chemical Engineering and Food Technologies, Wine and Agrifood
7 Research Institute (IVAGRO), Faculty of Sciences, University of Cadiz, 11510, Puerto
8 Real, Cádiz (Spain)

9

10 *Corresponding author:

11 Email: martin.ramirez@uca.es (M. Ramírez)

12

13

14 **Keywords:** biogas; elemental sulfur; CSTBR; hydrogen sulfide; autotrophic
15 denitrification; feedback control

16 *Abstract*

17 Biological desulfurization of biogas has been extensively studied using biotrickling filters
18 (BTFs). However, the accumulation of elemental sulfur (S^0) on the packing material
19 limits the use of this technology. To overcome this issue, the use of a continuous stirred
20 tank bioreactor (CSTBR) under anoxic conditions for biogas desulfurization and S^0
21 production is proposed in the present study. The effect of the main parameters (stirring
22 speed, N/S molar ratio, hydraulic residence time (HRT) and gas residence time (GRT))
23 on the bioreactor performance was studied. Under an inlet load (IL) of $100 \text{ g S-H}_2\text{S m}^{-3}$
24 h^{-1} and a GRT of 119 s, the CSTBR optimal operating conditions were 60 rpm, N/S molar
25 ratio of 1.1 and a HRT of 42 h, in which a removal efficiency (RE) and S^0 production of
26 $98.6 \pm 0.4\%$ and 88% were obtained, respectively. Under a GRT of 41s and an IL of 232
27 $\text{g S-H}_2\text{S m}^{-3} \text{ h}^{-1}$ the maximum elimination capacity (EC) of $166.0 \pm 7.2 \text{ g S-H}_2\text{S m}^{-3} \text{ h}^{-1}$
28 ($\text{RE} = 71.7 \pm 3.1\%$) was obtained. A proportional-integral feedback control strategy was
29 successfully applied to the bioreactor operated under a stepped variable IL.

30 **Keywords:** biogas; elemental sulfur; CSTBR; hydrogen sulfide; autotrophic
31 denitrification

32

33 **1.- Introduction.**

34 In a world with an ever-growing energy demand, the search for alternatives to the use of
35 fossil fuels has received much attention over the last two decades. The promotion of
36 renewable energy sources has been considered as an environmentally friendly and
37 sustainable solution to meet the needs of tomorrow's society [1]. Among other
38 renewable energy sources such as wind or solar energies, biogas has gained interest in
39 terms of its regular and predictable production flow rates [2].

40 After proper treatment, biogas can be used in electricity and heat generation using a
41 combined heat and power engine or as fuel in a solid oxide fuel cell [3]. Moreover, if the
42 methane (CH_4) concentration is increased, the upgraded biogas can be used as fuel for
43 vehicles or injected into gas grids [4]. Biogas, which is originated from the anaerobic
44 digestion of organic matter, is mainly composed of CH_4 , in a range of 55-75 vol%, and
45 carbon dioxide (CO_2), in the range of 30-45 vol%. The final composition of the biogas is
46 mainly dependent on the organic matter source and the digestion system. Apart from the
47 major components, biogas is composed of other trace pollutants. Among these, hydrogen
48 sulfide (H_2S), whose concentration in biogas can reach significant values ranging from
49 0.5 to 2 vol%, is widely considered to be the most toxic and corrosive and its mere
50 presence can severely limit biogas usage [5]. For example, it has to be removed from
51 biogas because, during combustion, the presence of H_2S can lead to harmful by-products
52 such as sulfur oxides (SO_x) and cause corrosion damage to equipment. Hence, biogas has
53 high energy content but must be desulfurized for its valorization.

54 H_2S can be removed from biogas by physico-chemical techniques (adsorption,
55 absorption, membrane separation, etc.) [6] or by biological techniques where
56 microorganisms degrade the pollutants. Nowadays, biological processes are considered
57 to be more environmentally friendly and cost-efficient [7]. So, their use has gained

58 interest over the last two decades. Traditionally, biological desulfurization has been
59 carried out by headspace micro aeration of digesters [8] and through the use of
60 biotrickling filters (BTFs) under aerobic or anoxic conditions using oxygen (O_2) or
61 nitrate/nitrite (NO_3^-/NO_2^-) as electron acceptors, respectively [9–14]. Despite the BTF
62 being shown to achieve high elimination capacities (ECs), robustness and cost-
63 effectiveness, a common drawback of its use in biological desulfurization is the
64 accumulation of elemental sulfur on the packing material. This sulfur aggregation,
65 provoked by working with low concentrations of the electron acceptor, results in pipe
66 clogging, which leads to higher pressure drops and system flooding, causing operation
67 shutdowns and high maintenance costs [15,16]. Sulfur production can be reduced by a
68 higher electron acceptor feeding rate favoring complete oxidation of sulfide to sulfate.
69 However, the production of sulfate as the main oxidation product of the anoxic
70 desulfurization is undesirable because firstly, its production entails a high operational cost
71 if commercial nitrate/nitrite is used, and secondly, it can be reduced again to sulfide under
72 anaerobic conditions [17]. Nevertheless, the operational costs can be greatly reduced if
73 the nitrate/nitrite is produced by nitrification of ammonium-rich wastewater [7]. The
74 partial oxidation of sulfide to sulfur is advantageous because it can be recovered from the
75 effluent by settling and used as an electron donor for autotrophic denitrification [18,19]
76 and as a renewable feedstock for the fertilizer and chemical industries [20].

77 A possible solution to overcome the main shortcomings of BTF usage for sulfur
78 production would be the use of suspended biomass bioreactors (SBB). Sulfur could be
79 recovered from these bioreactors because of the absence of support to which it would
80 otherwise become adhered. Some previous work on sulfide partial oxidation to sulfur in
81 SBBs has been carried out using oxygen as electron acceptor [21–23]. However, despite
82 the application of continuous SBBs to biological aerobic desulfurization of biogas being

83 widely investigated, scarce research has been conducted on the performance of the SBB
84 under anoxic conditions for biogas desulfurization. Anoxic desulfurization has some
85 advantages over the aerobic process such as the absence of biogas dilution, no oxygen
86 mass transfer limitation, reduction in explosion risks and a better N/S molar ratio
87 manipulation [11,24]. NO_2^- has been successfully used in BTFs [9] without reduction of
88 the H_2S removal efficiency (RE) ($94.74 \pm 0.01\%$). Bearing this in mind, the use of NO_2^-
89 is proposed in the present work as electron acceptor.

90 The main disadvantages of anoxic biodesulfurization versus the aerobic type are the
91 higher operation costs if the source of $\text{NO}_3^-/\text{NO}_2^-$ is a chemical reactant and the associated
92 storage risks. These problems could be solved by using an effluent from a nitrification
93 process. In this way, two toxic pollutants such as NH_4^+ and H_2S can be transformed into
94 harmless oxidation products such as N_2 and elemental sulfur. The production of NO_2^- by
95 partial nitrification over NO_3^- has several advantages such as lower operation costs (less
96 aeration is required) and its employment has been demonstrated to allow a faster growth
97 rate, and biological reaction, in the case of partial oxidation of sulfide to sulfur [25].
98 Whether chemically or biologically produced, the nitrite feeding has to be optimized in
99 order not to create extra costs and a sulfate- and nitrite-rich purge. In order to accomplish
100 this task, several feedback control strategies (e.g. on-off, proportional (P), proportional-
101 integral (PI) and proportional-integral-derivative (PID)) have been successfully applied
102 to anoxic desulfurization systems [26,27]. Among all these control strategies, PI control
103 mode stands as the most suitable for implementation in an anoxic biodesulfurization
104 process because results obtained by other researchers showed that its application led to
105 less oscillation in the nitrite feeding [27]. However, to the best of our knowledge, the
106 application of control strategies to the anoxic biodesulfurization in SBBs has not been
107 reported.

108 Low biomass concentration, high shear stress forces, or lower mass transfer rates are some
109 of the characteristic features of CSTBRs that widely differ from BTFs and which have
110 not been widely studied. Taking into consideration the aforementioned matters, the study
111 of the anoxic desulfurization process in a CSTBR becomes necessary to gain knowledge
112 about the effect of different operational parameters on the overall performance. Therefore,
113 the work reported here was aimed at studying the effect of the governing parameters in
114 the bioprocess, such as stirring speed, dilution rate (D), N/S molar ratio and gas residence
115 time (GRT) in order to optimize the bioprocess performance and enhance the sulfur
116 production.

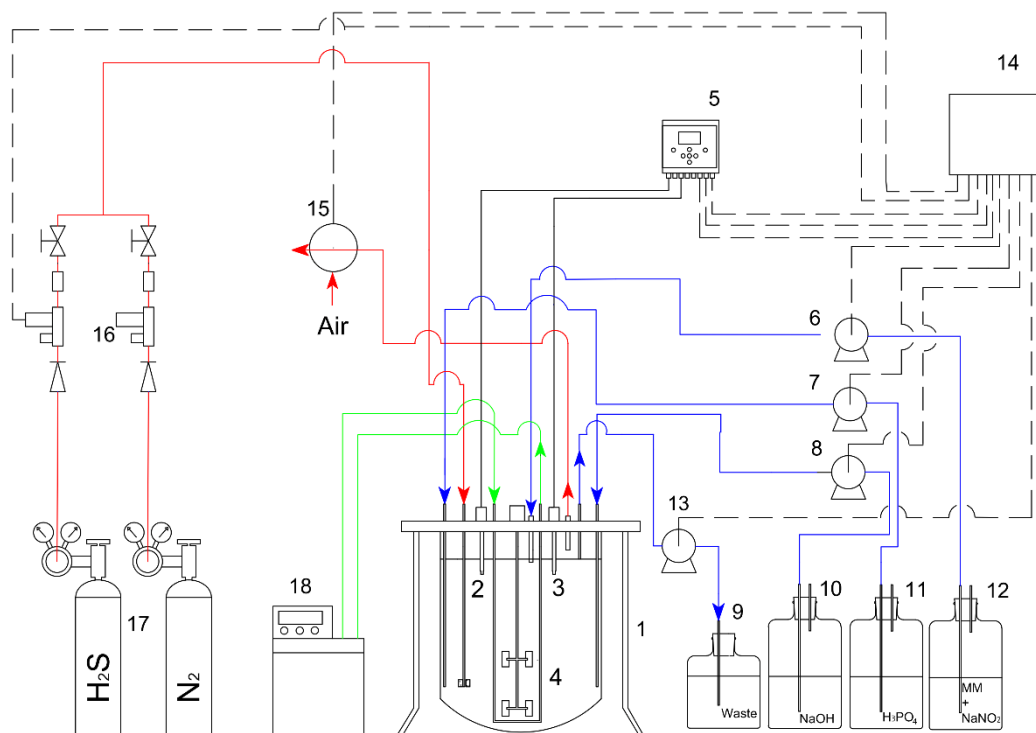
117 **2. Materials and Methods**

118 **2.1. Experimental Setup Description**

119 The experiments were carried out in a CSTBR (Applikon Biotechnology BV, The
120 Netherlands) with a working volume of 5.5 L (Fig. 1). The temperature was controlled by
121 a thermostat (RM6 Lauda, Germany) at 30°C. The bioreactor was fed with biogas
122 substitute (mixture of H₂S and N₂) controlled by two mass-flow controllers (F-201C,
123 Bronkhorst High-Tech B.V., The Netherlands). Oxidation-reduction potential (ORP) and
124 pH were measured with a multiparametric analyzer (Crison Multimeter 44, Hach Lange
125 S.L.U, Spain). The pH was set to 7.8 and controlled by the addition of H₃PO₄ (2N) and
126 NaOH (2N). The system was monitored and controlled using LabVIEW™ (Version 2015,
127 National Instruments™, USA).

128

129



130

131 **Fig. 1** Experimental setup. (1) CSTBR, (2) ORP probe, (3) pH probe (4) Stirrer, (5) Multimeter
 132 44, (6) Analog peristaltic pump, (7) H₃PO₄ peristaltic pump, (8) NaOH peristaltic pump, (9) Waste
 133 container, (10) NaOH container, (11) H₃PO₄ container, (12) Mineral medium + NaNO₂ container,
 134 (13) Discharge peristaltic pump, (14) PC and control system, (15) H₂S sensor, (16) Mass flow
 135 controllers, (17) Gas cylinders, (18) Thermostatic bath.

136

137 2.2. Mineral medium composition

138 The mineral medium was adapted from ATCC-1255 *Thiomicrospira denitrificans*
 139 medium [24] by enriching with NaNO₂ (1.74 – 3.12 g N-NO₂⁻ L⁻¹) and NaHCO₃ 1.89 (g
 140 L⁻¹) as carbon source.

141 2.3. Inoculum preparation

142 The bioreactor was inoculated with biomass from an anoxic BTF fed with nitrite used in
 143 previous works [27]. To desorb the microorganisms from the packing material, a selection
 144 of Pall rings was extracted from the top of the packed bed of the BTF. These were
 145 submerged in 200 mL of mineral medium and sonicated using an ultrasonic bath

146 (Ultrasons-H, Selecta, Spain) at 40 kHz for 15 min. The mineral medium with suspended
147 microorganisms was subsequently inoculated to the CSTBR.

148 **2.4. Reactor operation**

149 Throughout the long-term operation of the CSTBR (more than 160 days), a series of six
150 experiments was conducted. The main experimental conditions are listed in Table 1. All
151 the experiments were performed in continuous operation mode except Exp.1 which was
152 accomplished in batch mode.

153 Initially, a start-up period of 60 days was required to acclimatize the bacterial consortium
154 and find the proper conditions to grow it. Once the steady-state conditions were reached,
155 the experiments were conducted.

156 In Exp 1. the effect of stirring speed (under a constant IL of $70 \text{ g S-H}_2\text{S m}^{-3} \text{ h}^{-1}$) on H_2S
157 RE was studied. For nitrite feeding regulation, the automated feedback control mode
158 proposed by Almenglo et al. [15] was applied. Herewith, a concentrated nitrite solution
159 ($400 \text{ g NaNO}_2 \text{ L}^{-1}$) was discontinuously fed into the bioreactor using ORP measurement
160 as a control variable (Fig. S2, control loop 5). So, when nitrite concentration decreased in
161 the medium, H_2S started to accumulate in the broth leading to a sharp decrease in ORP.
162 Once the ORP value reached the set-point (-400 mV), 6 mL of the concentrated nitrite
163 solution was automatically supplied to the bioreactor. This addition, which caused a
164 nitrite concentration increase in the bioreactor up to $90 \text{ mg N-NO}_2 \text{ L}^{-1}$, led to an ORP
165 increase to normal working values (from -360 to -380 mV). Every 24 h the stirring speed
166 was stepwise increased by 50 rpm from 60 to 210 rpm while the $\text{H}_2\text{S}_{\text{out}}$ and ORP behavior
167 were monitored.

168 The effect of the N/S molar ratio on H_2S RE was studied in Exp. 2 at constant IL (100 g
169 $\text{S-H}_2\text{S m}^{-3} \text{ h}^{-1}$). The N/S molar ratio is the ratio between the amounts in moles of nitrogen

170 in the form of nitrite present in the liquid feed and sulfur in the form of sulfide present in
171 the biogas substitute. The outlet H₂S concentration was monitored while N/S molar ratio
172 values were changed every 2 h. Different N/S molar ratios were tested by modifying the
173 inlet flow of nitrite, which resulted in a HRT variation considered to be negligible due to
174 the short duration of the experiment.

175 Exp. 3 consisted of an optimization of the hydraulic retention time (HRT). Different HRT
176 values ranging from 55 to 30 h were studied under constant IL (100 g S-H₂S m⁻³h⁻¹) and
177 N/S molar ratio (1.1). The experiment lasted for 40 days, and was aimed at obtaining
178 consistent data at the steady-state. Conditions were maintained until the bioreactor was
179 considered to be at steady state, i.e. when changes in biomass concentration were close
180 to zero over a minimum of 3 times the HRT. Punctual measurements were performed to
181 monitor biomass concentration and sulfur production for ~5 days after the steady-state
182 condition was reached.

183 The influence of GRT was investigated in Exp. 4 for 48 h. Initially, under the previously
184 optimized experimental conditions of N/S molar ratio (1.1) and HRT (42 h), the inlet gas
185 flow was progressively increased every 2 h to test GRTs from 119 to 40 s keeping the IL
186 constant at 100 g S-H₂S m⁻³ h⁻¹ (Exp. 4.1). In this way, the [H₂S]_{in} decreased along the
187 duration of the experiment from 2500 to 853 ppm_v. In the second part of the experiment,
188 [H₂S]_{in} was kept constant at 2000 ppm_v while the GRT was lowered in the same way as
189 in Exp 4.1. Thus, the IL was increased from 79 to 232 g S-H₂S m⁻³ h⁻¹.

190 Finally, a PI feedback control was implemented in the system. Previous studies with
191 anoxic BTFs [26,27] demonstrated that the use of a PI control led to better stability of the
192 controlled variable compared with a PID strategy. In PI control the error between the set-
193 point and the controlled variable was used to calculate the proportional and integral terms.
194 By the calculus of these terms, the action to be applied to the manipulated variable, in this

195 case, the flow of the analog pump that feeds nitrite (Fig. S3, control loop 2), could be
196 determined. The method used to estimate the controller parameters as proportional gain
197 (k_p) and the integral time (τ_i) was the Ziegler-Nichols rule [28] based on step response.
198 Hence, the inlet H₂S concentration was increased by 20% from 2200 to 2640 ppm_v (IL
199 from 87 to 104 g S-H₂S m⁻³ h⁻¹). The graphical information obtained during this step-
200 response test in open-loop was used to determine the gain (K), delay time (L), and
201 constant time (T). K corresponds with the response increase while L and T were obtained
202 using the maximum slope tangent of the response curve. The k_p and τ_i constants were
203 determined using the mathematical equations Eq. 1 and Eq. 2 reported by Hägglund and
204 Åström [29]. The integral (k_i) gain was subsequently determined using Eq. 3 [28].

$$205 \quad k_p = \frac{0.9 T}{KL} \quad \text{Eq. 1}$$

$$206 \quad \tau_i = 3L \quad \text{Eq. 2}$$

$$207 \quad k_i = \frac{k_p}{\tau_i} \quad \text{Eq. 3}$$

208 Under this PI control, a profile of stepped variations in the IL (139.2 to 73.2 g S-H₂S m⁻
209 ³ h⁻¹) was applied to test the viability of the proposed control over an 8 day period.

210

211

212

213

214

215

216

217

218

219

220

221

222 **Table 1.** Operational conditions in the different experiments carried out.

Exp.	IL (gS-H ₂ S m ⁻³ h ⁻¹)	HRT(h)	GRT(s)	N/S molar ratio (mol:mol ⁻¹)	Stirring speed (rpm)	[H ₂ S] _{in} (ppm _v)	Studied Variable	Days
1	70	-	139	Variable	60 110 160 210	1800	Stirring speed	7
2	100	66 47 36 30	119	1.99 1.6 1.33 1.06 0.78	60	2500	N/S molar ratio	1
3	100	55 48 42 36 30	119	1.1	60	2500	HRT	40
4.1	100	42	119 104 89 73 57 41	1.1	60	2500 2171 1841 1512 1182 853	GRT (constant IL)	1
4.2	79 90 106 129 165 232	59 51 43 36 28 20	119 104 89 73 57 41	1.1	60	2000	GRT (constant [H ₂ S] _{in})	1
5	139-73	40-21.5	119	1.6-0.9	60	3500-1850	Stepwise changes in IL	3

223

224 **2.5. Analytical methods**

225 A biogas substitute (H₂S +N₂) was used to feed the system. The concentration of H₂S in
226 the inlet gas stream (>1000 ppm_v) was measured using a gas chromatograph (450-GC,
227 Bruker, Spain) with a thermal conductivity detector (TCD) and Poraplot Q plot FS 25 m
228 x 0.53 mm column. The oven temperature was set at 33 °C (2 min) and then increased
229 33–80 °C (10 °C min⁻¹), while the temperatures of the injector and detector were set at
230 150 °C. Samples with H₂S concentrations below 100 ppm_v were measured with a gas
231 chromatograph (450-GC, Bruker, Spain) equipped with a pulsed flame photometric
232 detector (PFPD) and Wcot Fused Silica 30m x 0.32 mm capillary column, under the

233 following experimental conditions; oven temperature: 35 °C (1.5 min), 33–80°C (15 °C
234 min⁻¹), injector temperature: 250 °C and detector temperature: 200 °C.

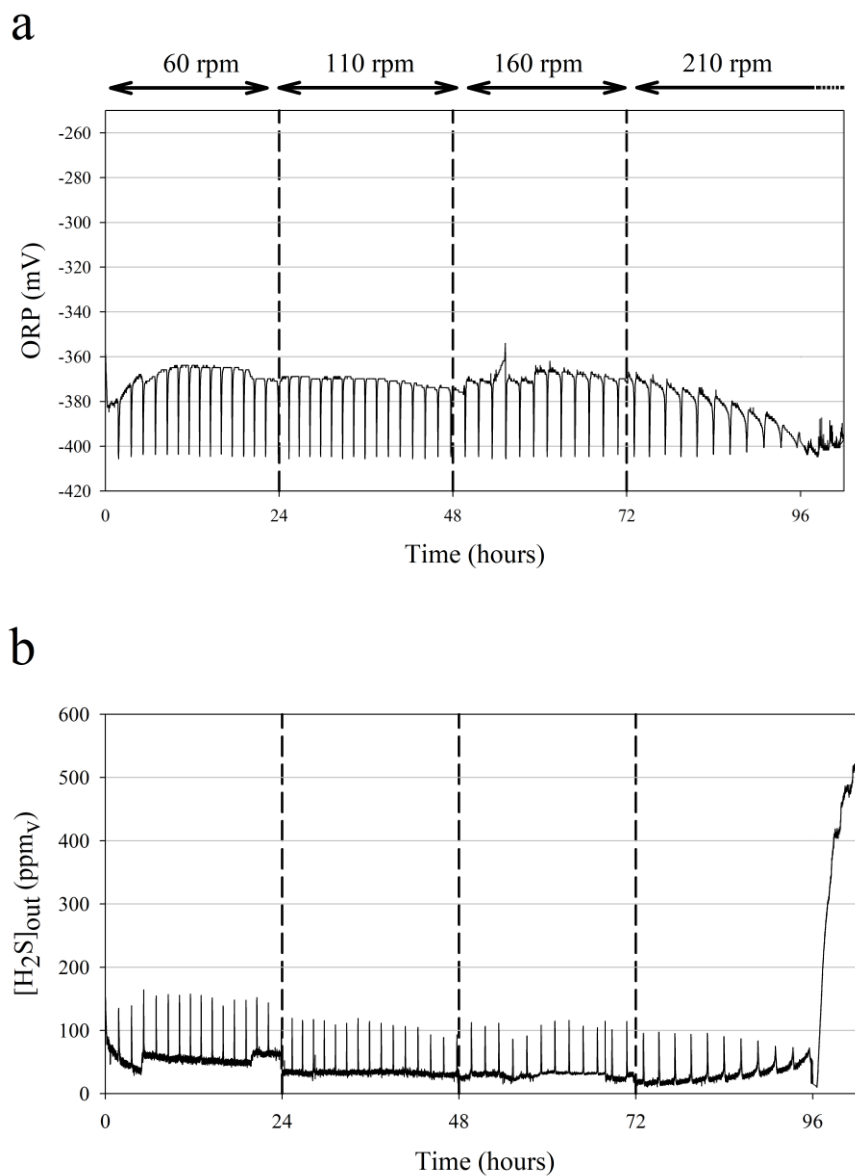
235 The CSTBR outlet gas stream was monitored using an electrochemical H₂S sensor
236 (SureCell, Euro-Gas Management Services, UK). Due to the electrochemical H₂S sensor
237 having a limited detection range of 0–200 ppm_v, the outlet gas stream was diluted with
238 air before passing through the sensor.

239 Samples were taken from the outlet liquid stream. Sulfate and nitrite were measured by a
240 turbidimetric method (4500-sulfate E) and a colorimetric method (4500-nitrite B),
241 respectively, according to the Standard Methods [30] using a Spectroquant® Pharo 300
242 spectrophotometer (Merck, Germany). Sulfur production was determined by making a
243 mass balance by subtraction [24]. Biomass concentration was determined by total
244 Kjeldahl nitrogen (TKN) using a Kjletec8200 Unit (Foss, Sweden). To perform this
245 analysis, 100 mL of the medium present in the CSTBR was centrifuged (13,100 x g, 6
246 min) and resuspended in distilled water twice to wash out the residual ammonium present
247 in the medium. Next, the pellet was transferred to a digestion tube in which 7 g of K₂SO₄
248 and 0.8 g of CuSO₄·5H₂O were added and dissolved into 12 mL of 95% (w/w) H₂SO₄.
249 Then, the sample was digested at 420 °C for 60 min. After digestion, the samples were
250 cooled to room temperature. Finally, the ammonium present in the digested samples was
251 transferred to a receiver solution (H₃BO₃ 4% (w/v)) by distillation (destilator Kjletec™
252 8200, Foss Iberia, S.A, Spain), using 80 mL of distilled water and 40% (w/w) NaOH. The
253 final amount of ammonium present in the sample was determined by acidometric titration
254 of the receiver solution with a standardized HCl solution (between 0.1 N and 0.2 N).

255 **3.- Results and discussion**

256 **3.1 Effect of the stirring speed on the RE**

257 In a CSTBR the stirring speed has a large influence on the mass transfer of compounds
258 from the gas phase to the liquid phase [31]. Using the experimental set-up described
259 above, when the stirring speed was increased while keeping the GRT constant (139 s),
260 the volumetric oxygen transfer coefficient (k_{La}) increased from 7.56 h^{-1} at 60 rpm to a
261 maximum of 14.94 h^{-1} at 210 rpm. The same test was performed using a realistic
262 concentration of elemental sulfur and no significant influence on the mass transfer from
263 gas to liquid phase was found (Fig. S1). Therefore, an improvement in the H_2S RE could
264 be expected by increasing the stirring speed.



265 **Fig. 2** - Profiles during Exp. 1 of: (a) ORP values; (b) H_2S concentration present in the outlet.

266

267 After inoculation, the CSTBR was operated for more than 60 days in order to obtain an
268 acclimatized biomass and reach a pseudo-steady state to start Exp. 1 (data not shown).
269 The effect of the stirring speed on the H_2S_{out} and ORP profiles is represented in Fig. 2.
270 These profiles are characteristic of the feedback control [9,15] operation mode previously
271 described in Section 2.4. Once nitrite was depleted, H_2S_{out} increased from 32.6 ± 11.9
272 ppm_v to $123.7 \pm 32.6 ppm_v$ and H_2S started to accumulate in the medium leading to a
273 rapid ORP decrease. When the ORP reached the set-point (-400 mV), the supplied nitrite
274 was immediately used by the bacterial consortium to degrade H_2S , restoring the H_2S_{out}
275 and ORP to normal working values. Fig. 2a shows how the ORP profiles were quite
276 similar when low stirring speeds (60-160 rpm) were applied, showing an average
277 of $-371.5 \pm 0.8 mV$. In contrast, when the bioreactor was operated at 210 rpm, ORP
278 working values started to decrease ($385.8 \pm 12.0 mV$), indicating sulfide accumulation in
279 the medium and leading to a working operation shutdown. Similar behavior was
280 identified when H_2S_{out} was analyzed (Fig. 2b). It remained approximately constant during
281 the first three stages ($41.3 \pm 16.9 ppm_v$). When the CSTBR was operated at 60, 110 and
282 160 rpm, the average H_2S_{out} ranged from $31.5 \pm 11.2 ppm_v$ to $58.0 \pm 11.9 ppm_v$. However,
283 when the stirring speed was increased to 210 rpm, the H_2S_{out} started to increase until a
284 large peak of H_2S up to $522.2 ppm_v$ was found in the outlet. At the end of the experiment,
285 aiming to gain insights into the ability of the biomass to recover from potential damage,
286 the CSTBR stirring speed was lowered to 110 rpm and a lower IL ($57 g S-H_2S m^{-3} h^{-1}$)
287 was applied to the bioreactor. Despite these “soft” conditions being maintained for three
288 days, the biomass was not able to recover forcing a re-inoculation of the bioreactor.

289 All these data indicate that the biomass present in the CSTBR responsible for the sulfide
290 oxidation is shear stress sensitive. The shear forces are mainly due to fluid-mechanical

291 stress induced directly by the stirring devices or by gas bubbles bursting [32]. An
292 acceptable estimation of the shear stress (τ_{Avg}) and rate (γ_{Avg}) coefficients for Newtonian
293 fluids could be made using their relation (Eq. 4) with viscosity (μ) and the Metzner and
294 Otto equation (Eq. 5), which has been demonstrated for Newtonian-fluids in laminar flow,
295 transitional flows, and a portion of the turbulent regime. K is the Metzner – Otto constant
296 and depends on the impeller.

$$297 \quad \tau_{Avg} = \mu \cdot \gamma_{Avg} \quad \text{Eq. 4}$$

$$298 \quad \gamma_{Avg} = K \cdot N \quad \text{Eq. 5}$$

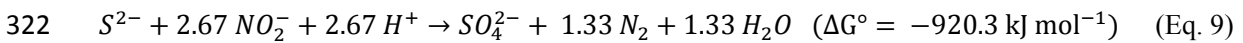
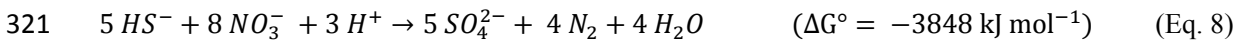
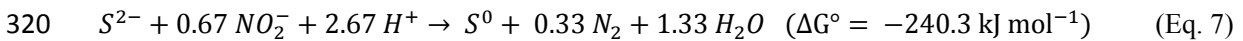
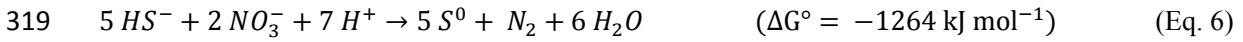
299 The γ_{Avg} near the Rushton impeller installed in the bioreactor ranged from 12 to 42 s⁻¹ at
300 60 and 210 rpm, respectively. The γ_{Avg} forces calculated are in line with those reported
301 in stirred vessels by Merchuk [33]. These γ_{Avg} corresponded to τ_{Avg} which ranged from
302 0.012 to 0.042 Pa. Many anaerobic bacteria are shear sensitive [34], but damage usually
303 occurs at higher agitation rates than those used in this study [35,36]. Therefore, the present
304 bacterial consortium seems to be especially sensitive to these forces. Possible solutions
305 to avoid causing damage to the bacterial consortium could be a reduction of the stirring
306 speed, which would in turn decrease the energy requirements of the bioreactor, or the use
307 of stirrers designed to minimize shear forces.

308 **3.2 Effect of N/S molar ratio on RE**

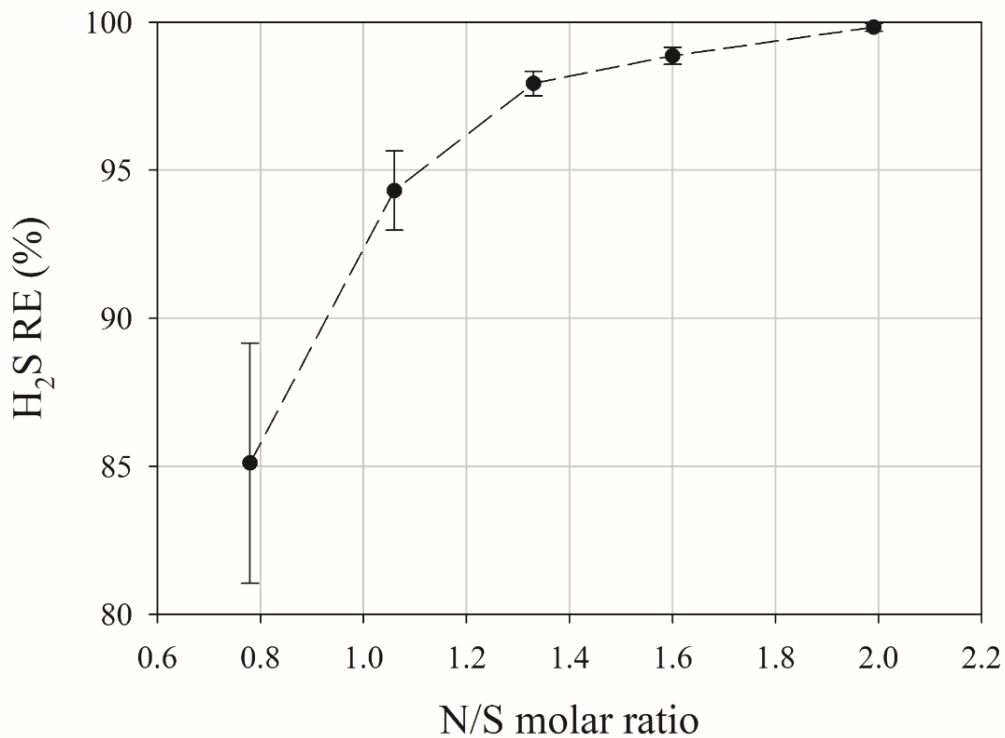
309 Determination of the optimal N/S molar ratio is essential because of its great influence
310 on the product selectivity and H₂S RE. Since elemental sulfur is the desired oxidation
311 product and most authors report that low N/S molar ratios favor the production of
312 elemental sulfur over sulfate [37–39], Exp. 2 was aimed at finding the lowest N/S molar
313 ratio without a decrease in the H₂S RE. At a constant IL of 100 g S-H₂S m⁻³ h⁻¹, H₂S_{out}

314 concentration values were monitored while the N/S molar ratios were progressively
 315 lowered.

316 Average H₂S RE values versus the different N/S molar ratios are shown in Fig. 3. N/S
 317 molar ratio determines the sulfur selectivity [24,40,41]. Low N/S molar ratio values favor
 318 elemental sulfur production (Eqs. 6 and 7) over sulfate (Eqs. 8 and 9) [37].



323 These experiments revealed that N/S molar ratios did indeed affect the H₂S RE in contrast
 324 to the behavior observed in BTFs. In BTFs, the N/S molar ratio can be reduced below the
 325 theoretical needs, which are 0.4 and 0.6 mol mol⁻¹ for nitrate and nitrite, respectively,
 326 without a significant decrease in the H₂S RE [9,41].



327

328 **Fig. 3** - Removal efficiencies at different N/S molar ratios (Exp. 2).

329

330 Different N/S molar ratios of 1.99, 1.6, 1.33, 1.1, and 0.78 mol mol⁻¹ were tested. The
331 H₂S RE depends on the mass transfer of the pollutant, which is related to the k_{LA} and the
332 chemical characteristics of the H₂S, and the microbial activity. An increase in pH leads
333 to greater solubility of H₂S and, therefore, a greater mass transfer. When the highest N/S
334 molar ratio was applied (1.99), the H₂S RE was 99.8%. This high H₂S RE proved that
335 there were no limitations on the mass transfer of the pollutant contained in the biogas to
336 the liquid at these conditions. When the highest N/S molar ratio was applied (1.99), the
337 H₂S RE was 99.8%. This result highlights the low mass transfer limitation of the pollutant
338 from the biogas stream to the medium under these conditions. When N/S molar ratio was
339 lowered to 1.1 mol mol⁻¹, the H₂S RE was affected leading to a reduction to 94.2%.
340 Finally, the lowest N/S molar ratio used (0.78) led to an average H₂S RE drop to 84.9%
341 causing instability in the system.

342 This relationship between N/S molar ratios and H₂S RE was previously reported in the
343 literature in SBB for biogas desulfurization. Dolejs et al. [42] reported that N/S molar
344 ratio was decisive for the efficiency of a CSTBR removing H₂S using NO₃⁻ as the main
345 electron acceptor. In the same study, a sulfide RE drop from 96% to 55% was found when
346 the N/S molar ratio was reduced from 1.18 to 0.36. Another study performed by Li et al.
347 [40] found that, while a decrease in the N/S molar ratio did not affect the H₂S removal by
348 a BTF, the same low N/S molar ratio values diminished H₂S RE in a bubble column.
349 These differences were explained because of the vastly different mass transfer rates
350 between both types of bioreactors [43].

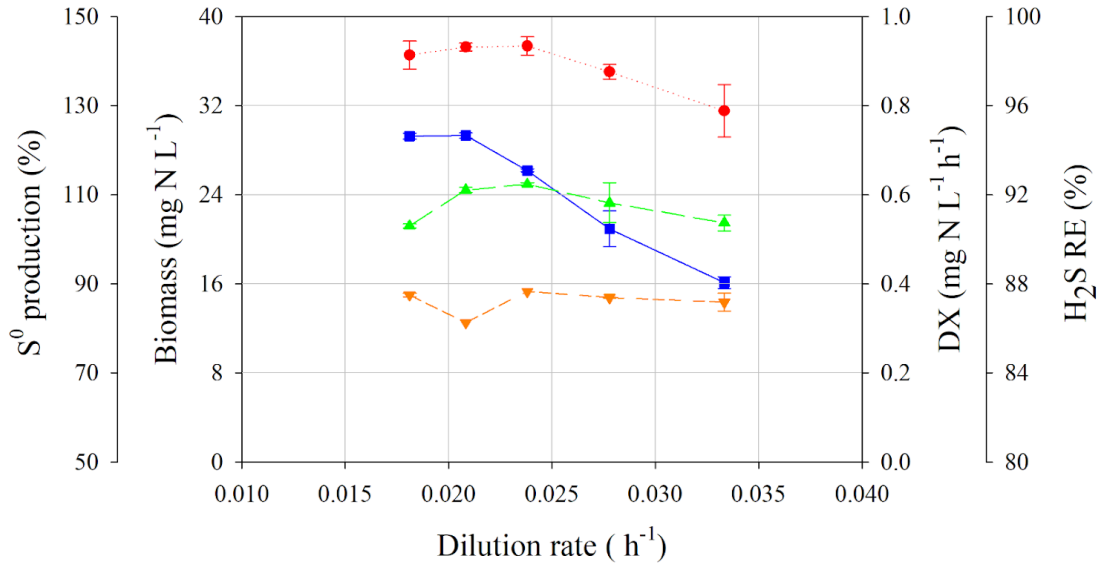
351 However, in this experiment we can assume that the low H₂S RE found at the lowest N/S
352 molar ratio tested cannot be explained by a mass transfer limitation because the ORP

353 decreased from -306 mV to -422 mV and the operational conditions (i.e. stirring speed
354 and GRT) remained constant during the whole experiment (data not shown). The ORP
355 decrease could be explained by a higher presence of HS⁻ ions in the medium, indicating
356 that mass transfer was not limited. A biomass concentration decrease could not be
357 responsible for the worse performance shown at the lowest N/S molar ratios tested. The
358 biomass concentration could be assumed to be constant due to the short duration of the
359 experiment. Therefore, the only reason that could explain the poor H₂S RE at N/S molar
360 ratios below 1.1 mol mol⁻¹ is that the amount of nitrite supplied to the bacteria at these
361 N/S ratios was insufficient to carry out the biological desulfurization. According to the
362 stoichiometric equations of sulfide oxidation using nitrite (Eqs. 7 and 9), N/S molar ratios
363 of 0.67 and 2.67 mol mol⁻¹ are required to achieve the partial oxidation of H₂S to
364 elemental sulfur and the complete oxidation to sulfate, respectively. Our data are in
365 complete agreement with those obtained by Mahmood et al. [44], who used the same N/S
366 molar ratio (1.1) to operate an anoxic desulfurization bioreactor using nitrite as electron
367 acceptor. In that study, sulfide REs over 95% were also obtained using that N/S molar
368 ratio and sulfate was again obtained as a minor product (~25%). The formation of sulfate,
369 as has been demonstrated in Exp. 3, is difficult to avoid and causes an increase in the
370 required N/S molar ratio of the bioprocess.

371 **3.3 Effect of HRT on process performance**

372 HRT or dilution rate (D) is an important parameter to optimize in most CSTBRs due to
373 its large influence on the bioreactor performance. The biomass productivity, i.e. dilution
374 rate times biomass concentration (DX), is a well-known parameter used to determine the
375 optimal HRT or dilution rate of the bioprocess. At the dilution rate in which the
376 production rate of biomass per unit reactor volume is considered to be maximum
377 (maximum DX product value), the H₂S EC is expected to be the highest. Therefore, this

378 test was aimed at studying and optimizing the effect of dilution rate on biomass
 379 concentration and productivity, H₂S RE, and sulfur production.



380

381 **Fig. 4** – DX product (green triangle), biomass concentration (blue square), H₂S removal
 382 efficiency (red circle), and sulfur production (orange inverted triangle) versus dilution rate (Exp.
 383 3).

384

385 In order to study the effect of dilution rate on biomass production and RE, Exp. 3 was
 386 carried out for 40 days. Initially, at the lowest D tested of 0.018 and 0.021 h⁻¹ (HRTs of
 387 55 and 48 h, respectively), the biomass hardly changed indicating that the maximum
 388 biomass concentration was reached (29.3 ± 0.4 mg N L⁻¹). An increase of dilution rate
 389 from 0.021 to 0.033 h⁻¹ led to a proportional decrease in biomass concentration from
 390 29.35 to 16.11 mg N L⁻¹. Hence, a DX curve could be made, and is presented in Fig. 4 as
 391 green triangles. This curve has a maximum DX value of 0.63 mg N L⁻¹ h⁻¹ at a dilution
 392 rate of 0.024 h⁻¹, which corresponds to an HRT of 42 h. From these data collected at
 393 pseudo-steady state, the biomass growth yield ($Y_{X/S^{2-}}$) was also calculated (Eq. S1). An
 394 average $Y_{X/S^{2-}}$ of 0.05 ± 0.003 g VSS (g S²⁻)⁻¹ was calculated assuming C₅H₇O₂N as
 395 typical biomass composition [25]. Mora et al. [25] reported a higher $Y_{X/S^{2-}}$ of 0.328 ±

396 0.045 g VSS (g S^{2-})⁻¹ compared to the one obtained in the present work, which could
397 probably be explained by the different compositions of the bacterial consortia.

398 H₂S REs were slightly affected under the different conditions tested during Exp. 3 (Fig.
399 4, red circles). The lowest average RE value ($\text{RE} = 95.8 \pm 1.2\%$) was found when the
400 highest dilution rate was applied to the bioreactor ($D = 0.033 \text{ h}^{-1}$; HRT = 30 h). On the
401 other hand, the best performance ($\text{RE} = 98.6 \pm 0.4 \%$) was found when the highest DX
402 product was obtained, at a dilution of 0.024 h^{-1} (HRT = 42 h). These data lend support to
403 previous findings in the literature. Mahmood et al. [44] reported that the effect of HRTs
404 ranging from 36 to 2.4 h had little impact on the H₂S RE, which ranged from 99.8 to
405 99.2%, of an airlift bioreactor using nitrite as the main electron acceptor. Also, Can-
406 Dogan et al. [45] found that HRTs from 86.4 to 2h did not affect the sulfide RE, which
407 always exceeded 92%.

408 Additionally, the influence of the HRT on sulfur production at the previously optimized
409 N/S molar ratio in Exp. 2 (1.1 mol mol^{-1}) was studied. As in the case of H₂S RE, the
410 sulfur production percentages were modestly influenced by HRT ranging from 81.3% to
411 88.3%. The highest sulfur production was found at a dilution rate of 0.024 h^{-1} (HRT = 42
412 h). These high values of sulfur production give an explanation to the milky yellow/white
413 appearance of the bioreactor (Fig. S4) when low N/S molar ratios were applied. This
414 characteristic appearance was previously linked, in the literature, with the accumulation
415 of sulfur particles [46,47]. Despite sulfide removal by autotrophic denitrification having
416 been carried out in SBBs, sulfur production data have not been widely reported. Most
417 studies claim that sulfur accumulates in the bioreactor when working at low N/S molar
418 ratios but scarce further data are given [42,47,48].

419 Mahmood et al. [44] reported that sulfur was obtained as the main oxidation product
420 (around 66%) in a UASB reactor using nitrite as electron acceptor. Compared to aerobic

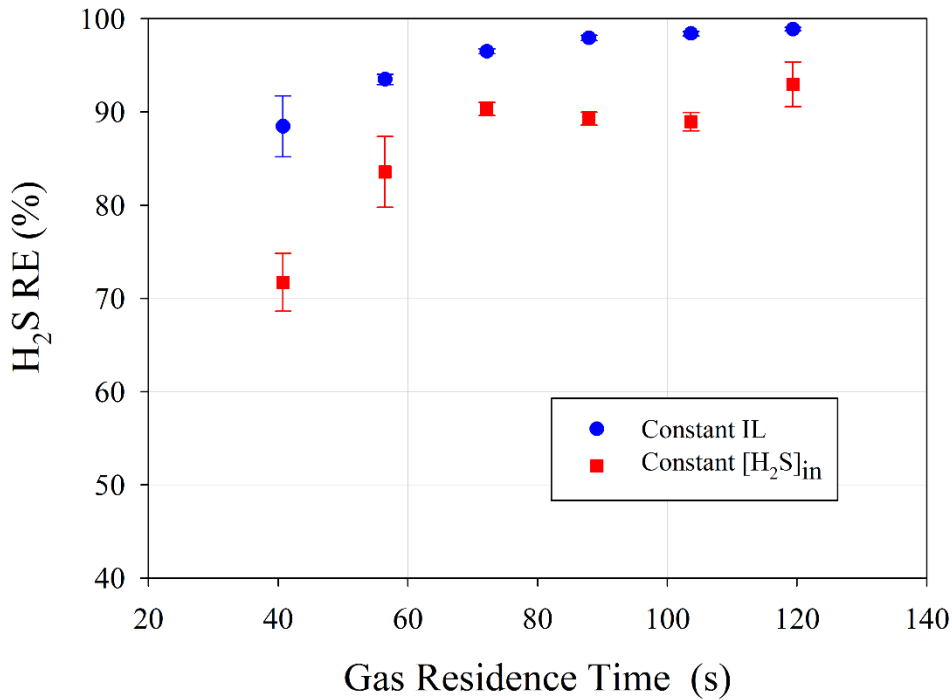
421 SBB, as happens in anoxic desulfurization, the limitation of the electron acceptor
422 enhances the sulfur production. For example, Lohwacharin and Annachatre [22] and
423 Buisman et al. [21] reported that up to 90% of sulfide removed was converted to sulfur
424 in an airlift bioreactor operating under oxygen-limited conditions. Also, a similar value
425 of sulfur production (87.76%) was found under optimal operational conditions by Roosta
426 et al. [49] using a model validated with an aerobic CSTBR. Lower values of sulfur
427 production (65%) were obtained by Krishnakumar et al. [23] with an aerobic reverse
428 fluidized loop reactor under high sulfide loads. Even though working at low N/S molar
429 ratios is not feasible in BTFs because of the column clogging problems caused by sulfur
430 accumulation, some studies are available. Cano et al. [41] obtained sulfur production up
431 to 99% at N/S molar ratios as low as 0.34 using NO_3^- as electron acceptor. Brito et al. [9]
432 obtained sulfur as the main oxidation product using a BTF fed with nitrite at N/S molar
433 ratios ranging from 1.1 to 1.5. Also, Montebello et al. [50] obtained sulfur production
434 rates ranging from 20 to approximately 60% using an aerobic BTF operating under acidic
435 conditions.

436 Despite neither H_2S RE nor sulfur production differences among dilution rates being
437 substantial, in the present study, taking into consideration that the best performance in
438 terms of H_2S removal and sulfur production was obtained when the maximum DX product
439 was found, subsequent experiments were conducted considering a D of 0.024 h^{-1} (HRT
440 = 42 h) as optimum.

441 **3.4 Effect of GRT**

442 Among all parameters affecting bioreactor efficiency, the gas flow rate, which determines
443 GRT, stands as one of the most important design parameters to optimize. Lower GRTs
444 are strongly correlated with smaller bioreactors as well as lower costs of construction,
445 maintenance, and operation. Decreasing the GRT results in an increase of the pollutant

446 loading rate to the CSTBR, and therefore the number of pollutants that can potentially be
447 removed. So, in order to study the effect of the GRT on H₂S removal by the CSTBR, two
448 different experiments were carried out (Exp 4.1 and 4.2).



449

450 **Fig. 5** – Removal Efficiency versus Gas Residence Time keeping constant: (1) Inlet Load (blue
451 circles) and; (2) Inlet H₂S concentration (red squares).

452

453 Initially, when the IL was kept constant and GRT and [H₂S]_{in} decreased in Exp. 4.1 (Fig.
454 5, blue circles), REs of $88.5 \pm 3.3\%$ and $93.4 \pm 0.6\%$ were obtained at the lowest GRTs
455 tested (41 and 56 s, respectively). Nonetheless, once GRT was increased to 72 s, RE
456 increased to $96.5 \pm 0.3\%$ revealing this GRT as a suitable choice to obtain REs above
457 95%. As expected, when GRT was further increased, REs in turn increased up to a
458 maximum of 98.9 ± 0.2 at the highest GRT tested (119 s). Secondly, in Exp. 4.2 (Fig. 5,
459 red squares) the same GRTs were tested but, this time, keeping the H₂S inlet concentration
460 constant at 2,000 ppm_v, which in turn led to an IL increase from 90 to 232 g S-H₂S m⁻³
461 h⁻¹. This time, the differences between GRTs are more remarkable. At the highest IL (232

462 g S-H₂S m⁻³ h⁻¹) and the lowest GRT (41 s) the maximum EC in the present study was
463 found (EC = 166.0 ± 7.2 g S-H₂S m⁻³ h⁻¹; RE = 71.7 ± 3.1%). When the GRT was
464 increased, slight differences were found at GRTs ranging from 72 to 104 s where an
465 average RE of 89.5 ± 0.6% occurred. Finally, the maximum RE in Exp. 4.2 (93.0 ± 2.4%)
466 was obtained at the highest GRT of 119 s (IL = 79.0 g S-H₂S m⁻³ h⁻¹).

467 Comparison of these data with the literature is difficult because of the few studies about
468 the GRT effect in SBB for hydrogen sulfide removal. Most of the research on H₂S
469 removal in SBBs has been conducted using a sulfide salt solution as substrate so the
470 influence of GRT has not been widely studied. In this way, additional external absorption
471 units would be required for the operation of these bioreactors, involving extra capital and
472 operating costs. Amongst the authors who have used gas effluents with H₂S, Zytoon et al.
473 [51] fed an airlift bioreactor with a mixture of air and H₂S corresponding to a GRT of
474 1484 s. Also, a GRT of 300 s was applied by Li et al. [40] in a bubble column carrying
475 out anoxic desulfurization, achieving REs ranging from 66.2% to 99.6% under an IL
476 around 30 g S-H₂S m⁻³ h⁻¹.

477 In comparison with BTFs, Cano et al. [41] were able to achieve H₂S REs between 96-
478 98.5% in a BTF operating at empty bed residence times (EBRTs) ranging from 32 to 42
479 s and the same inlet H₂S concentration as used in this study (2,000 ppm_v). This better
480 performance shown by the BTF mentioned above could be explained in terms of its high
481 height/diameter ratio (9.8), which allowed it to obtain higher mass transfer rates.
482 Moreover, BTFs are capable of hosting large amounts of biomass fixed to the packing
483 material, which leads to higher substrate consumption rates in BTFs in comparison to
484 CSTBRs. However, the performance of other anoxic BTFs was affected at higher EBRTs
485 than those tested in the present study, probably due to the lower height/diameter ratios
486 compared to Cano et al. [41]. For example, Almenglo et al. [52] obtained a RE drop from

487 99% to 80% when the EBRT was decreased from 601 to 137 s. Also, the H₂S RE was
488 greatly affected by EBRT in another anoxic BTF when EBRT was diminished from 121
489 s (RE = 98%) to 30 s (RE = 47%) [11].

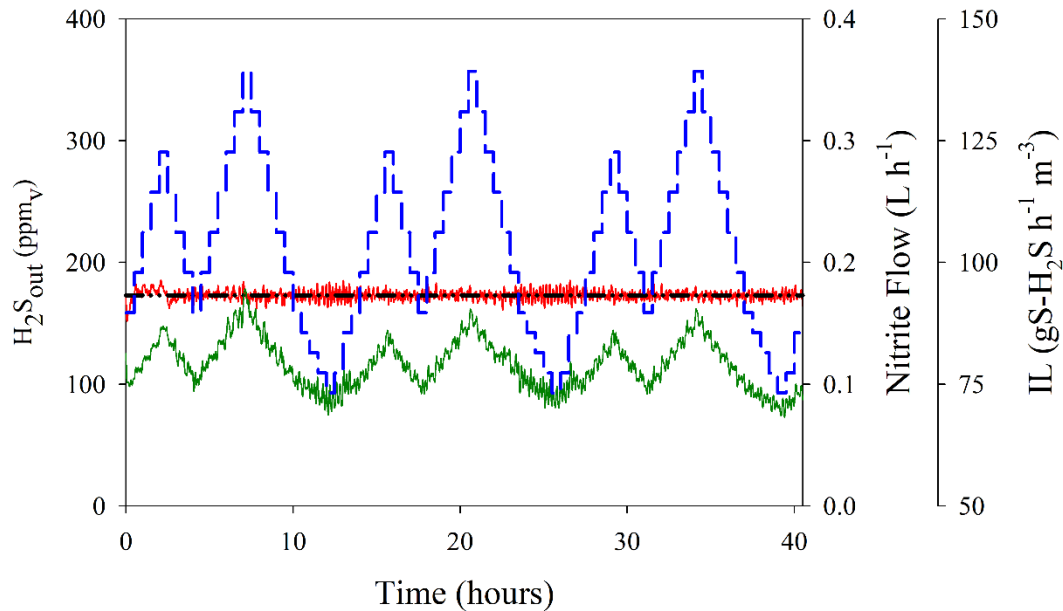
490 The maximum EC obtained in the present study (EC = 166.0 ± 7.2 g S-H₂S m⁻³ h⁻¹; RE
491 = 71.7 ± 3.1%) improves on the performance of most SBBs removing H₂S from biogas
492 that have been reported in the literature. ECs around 25 g S-H₂S m⁻³ h⁻¹ (RE = 99.6 ±
493 0.4%) were obtained in an anoxic bubble column under a GRT of 300 s [40]. A maximum
494 EC of 113 g S-H₂S m⁻³ h⁻¹ (RE ≈ 95%) was achieved by Zytoon et al. [51] in a pilot-scale
495 airlift aerobic bioreactor at a GRT of 1484 s. Jiang et al. (2020) obtained a higher (EC
496 256 g S-H₂S m⁻³ h⁻¹) refluxing the outlet gas in an aerobic biological bubble column but
497 with a much lower RE of 57%. Similar or better results were obtained in aerobic or anoxic
498 bioreactors removing sulfide from wastewaters [23,44,46,54]. Also, the EC values
499 obtained in the present study exceed the performance of several BTFs at comparable
500 EBRTs [26,52,55,56]. Despite there being some BTFs that have higher ECs [33,48], the
501 accumulation of elemental sulfur in the packing material would limit its application.

502 Therefore, it can be concluded that the H₂S RE values obtained from the studied CSTBR
503 were better than those from other suspended biomass bioreactors and are in line with
504 BTFs carrying out the anoxic desulfurization.

505 **3.5 Use of PI control under stepped variation**

506 In the last part of the study, the effect of inlet perturbation on H₂S RE under a PI control
507 was studied. First of all, a suitable set of gain parameters had to be obtained in order to
508 implement a convenient and robust control. Brito et al. [26] applied different feedback
509 control strategies to an anoxic desulfurization system and concluded that a PI controller
510 had a more stable behavior at different ILs than a PID controller. Therefore, in the present

511 work, a PI control was implemented. Due to its responsiveness, simplicity and adequacy,
 512 the tuning method used was the Ziegler-Nichols rule based on step response [27]. The
 513 final values for the different gain parameters were $K_p = 0.104$ and $K_i = 0.0005$.



514

515 **Fig. 6** – H_2S concentration present in the outlet (red) and set-point (black) under stepped
 516 variations in IL (blue). Nitrite inlet flow is represented in green.

517

518 Then, once the PI controller was implemented, the effect of a stepped inlet perturbation
 519 (Fig. 6, blue line) on the CSTBR under PI control was studied (Exp. 5). The results of
 520 this experiment are depicted in Fig. 6. The H_2S set-point selected was 173 ppm_v. This set-
 521 point was chosen because the outlet biogas from this bioreactor could be fed to an internal
 522 combustion engine, whose technical limit is 200 ppm_v [58]. The average H_2S outlet
 523 concentration was 173 ± 6.7 ppm_v. These results concur well with the data depicted in
 524 Fig. 6, in which it can be seen that the PI control successfully maintained the H_2S outlet
 525 concentration (Fig. 6, red line) near the set-point (Fig. 6, black line). The feedback control
 526 allowed us to adjust the outlet H_2S concentration by modifying the nitrite flow rate (Fig
 527 6, green line) resulting in an average of 0.116 ± 0.021 L h⁻¹. Despite the N/S molar ratio
 528 varying throughout the experiment, these changes were not excessive and the N/S molar

529 ratio was kept almost constant to an average of 1.1 ± 0.1 . This N/S molar ratio, applied
530 by the automated feedback controller, ended up being the same as the previously
531 optimized value in Exp 2. Herewith, the average RE of the whole experiment was $93.4 \pm$
532 0.3% which satisfactorily met the requirements of the system.

533 The application of feedback control strategies to a SBB for sulfide removal has not been
534 reported previously. The studies carried out previously in anoxic BTFs used manual,
535 programmed and continuously modulated control [15,26,27]. Manual feeding of nitrate
536 is possible but not feasible in an industrial bioreactor due to the high operational costs
537 and underperformance [26]. An automated method to supply nitrate was proposed by
538 Almenglo et al. [15] by measuring ORP in the same way as Exp. 1. Even though this
539 control strategy had already been applied in the pilot-scale, high concentrations of nitrate
540 were found in the recirculation medium outlet stream in addition to not being able to
541 prevent outlet peaks of H_2S in the outlet gas stream when nitrate was depleted. Different
542 feedback strategies have also been applied to anoxic and aerobic BTFs for H_2S removal
543 [26,27,39]. PID control using the H_2S outlet concentration as controlled variable was
544 successfully applied to an anoxic BTF fed with nitrate to a set-point of 100 ppm_v . This
545 control strategy maintained an average offset of $\pm 7 \text{ ppm}_v$ under similar stepwise
546 variations in IL. In another study, a PI control was successfully applied to an anoxic BTF
547 for H_2S removal and tested under remarkably variable ILs ranging from 28 to 141 g S-
548 $\text{H}_2\text{S m}^{-3} \text{ h}^{-1}$ [27]. Here, the PI control satisfactorily maintained the H_2S outlet
549 concentration between 90 and 114 ppm_v using a set-point of 100 ppm_v .

550 Therefore, taking into consideration the above, the CSTBR stands as a favorable
551 alternative to BTFs to maintain a stable H_2S concentration in the outlet under variable
552 ILs.

553

554 **4.- Conclusion.**

555 The use of a CSTBR to carry out the anoxic biogas desulfurization offers an alternative
556 to the BTF. The optimal conditions to maximize elemental sulfur production without
557 decreasing the H₂S RE at an IL of 100 g S-H₂S m⁻³ h⁻¹ were: 60 rpm, HRT of 42 h, N/S
558 molar ratio of 1.1 and GRT of 119 s, obtaining an H₂S RE of 98.6 ± 0.4 % and 88% of
559 sulfur production. The maximum EC obtained was 166.0 ± 7.2 g S-H₂S m⁻³ h⁻¹ (RE =
560 71.7 ± 3.1%) operating at a GRT of 41 s. The PI feedback control was able to keep the
561 actual outlet concentration very stable and close to the set-point.

562 **Acknowledgments**

563 This work was financially supported by the Spanish Government (Ministerio de
564 Economía y Competitividad) [grant number CTM2016-79089-R] and by the University
565 of Cadiz which provided financial support through the PIF UCA/REC01VI/2017.

566 **References**

- 567 [1] I. Angelidaki, L. Treu, P. Tsapekos, G. Luo, S. Campanaro, H. Wenzel, P.G.
568 Kougias, Biogas upgrading and utilization: Current status and perspectives,
569 Biotechnol. Adv. 36 (2018) 452–466.
570 <https://doi.org/10.1016/j.biotechadv.2018.01.011>.
- 571 [2] C. Agustini, M. da Costa, M. Gutterres, Biogas production from tannery solid
572 wastes – Scale-up and cost saving analysis, J. Clean. Prod. 187 (2018) 158–164.
573 <https://doi.org/10.1016/j.jclepro.2018.03.185>.
- 574 [3] M. Ramírez, J.M. Gómez, D. Cantero, Biogas: Sources, Purification and Uses, in
575 Energy Science and Technology Vol. 11. Hydrogen and Other Technologies;
576 Sivakumar, S., Sharma, U.C, Prasad, R., Eds., Studium Press LCC, USA, (2015)
577 pp 296–323.
- 578 [4] F.M. Baena-Moreno, M. Rodríguez-Galán, F. Vega, L.F. Vilches, B. Navarrete,
579 Review: recent advances in biogas purifying technologies, Int. J. Green Energy.

- 580 16 (2019) 401–412. <https://doi.org/10.1080/15435075.2019.1572610>.
- 581 [5] O.A. Habeeb, R. Kanthasamy, G.A.M. Ali, S. Sethupathi, R.B.M. Yunus,
582 Hydrogen sulfide emission sources, regulations, and removal techniques: A
583 review, *Rev. Chem. Eng.* 34 (2018) 837–854. [https://doi.org/10.1515/revce-](https://doi.org/10.1515/revce-2017-0004)
584 2017-0004.
- 585 [6] M.S. Shah, M. Tsapatsis, J.I. Siepmann, Hydrogen Sulfide Capture: From
586 Absorption in Polar Liquids to Oxide, Zeolite, and Metal-Organic Framework
587 Adsorbents and Membranes, *Chem. Rev.* 117 (2017) 9755–9803.
588 <https://doi.org/10.1021/acs.chemrev.7b00095>.
- 589 [7] P.I. Cano, J. Colón, M. Ramírez, J. Lafuente, D. Gabriel, D. Cantero, Life cycle
590 assessment of different physical-chemical and biological technologies for biogas
591 desulfurization in sewage treatment plants, *J. Clean. Prod.* 181 (2018) 663–674.
592 <https://doi.org/10.1016/j.jclepro.2018.02.018>.
- 593 [8] A. Giordano, F. Di Capua, G. Esposito, F. Pirozzi, Long-term biogas
594 desulfurization under different microaerobic conditions in full-scale thermophilic
595 digesters co-digesting high-solid sewage sludge, *Int. Biodeterior. Biodegrad.* 142
596 (2019) 131–136. <https://doi.org/10.1016/j.ibiod.2019.05.017>.
- 597 [9] J. Brito, A. Valle, F. Almenglo, M. Ramírez, D. Cantero, Progressive change
598 from nitrate to nitrite as the electron acceptor for the oxidation of H₂S under
599 feedback control in an anoxic biotrickling filter, *Biochem. Eng. J.* 139 (2018)
600 154–161. <https://doi.org/10.1016/j.bej.2018.08.017>.
- 601 [10] M. Fortuny, J.A. Baeza, X. Gamisans, C. Casas, J. Lafuente, M.A. Deshusses, D.
602 Gabriel, Biological sweetening of energy gases mimics in biotrickling filters,
603 *Chemosphere.* 71 (2008) 10–17.
604 <https://doi.org/10.1016/j.chemosphere.2007.10.072>.
- 605 [11] A.M. Montebello, M. Fernández, F. Almenglo, M. Ramírez, D. Cantero, M.
606 Baeza, D. Gabriel, Simultaneous methylmercaptan and hydrogen sulfide removal
607 in the desulfurization of biogas in aerobic and anoxic biotrickling filters, *Chem.*
608 *Eng. J.* 200–202 (2012) 237–246. <https://doi.org/10.1016/j.cej.2012.06.043>.
- 609 [12] G. Soreanu, M. Béland, P. Falletta, K. Edmonson, P. Seto, Investigation on the
610 use of nitrified wastewater for the steady-state operation of a biotrickling filter

- 611 for the removal of hydrogen sulphide in biogas, *J. Environ. Eng. Sci.* 7 (2008)
612 543–552. <https://doi.org/10.1139/S08-023>.
- 613 [13] W. Watsuntorn, R. Khanongnuch, W. Chulalaksananukul, E.R. Rene, P.N.L.
614 Lens, Resilient performance of an anoxic biotrickling filter for hydrogen sulphide
615 removal from a biogas mimic: Steady, transient state and neural network
616 evaluation, *J. Clean. Prod.* 249 (2020) 119351.
617 <https://doi.org/10.1016/j.jclepro.2019.119351>.
- 618 [14] R. Khanongnuch, F. Di Capua, A.M. Lakaniemi, E.R. Rene, P.N.L. Lens,
619 Transient–state operation of an anoxic biotrickling filter for H₂S removal, *J.*
620 *Hazard. Mater.* 377 (2019) 42–51. <https://doi.org/10.1016/j.jhazmat.2019.05.043>.
- 621 [15] F. Almenglo, M. Ramírez, J.M. Gómez, D. Cantero, Operational conditions for
622 start-up and nitrate-feeding in an anoxic biotrickling filtration process at pilot
623 scale, *Chem. Eng. J.* 285 (2016) 83–91. <https://doi.org/10.1016/j.cej.2015.09.094>.
- 624 [16] X. Qiu, M.A. Deshusses, Performance of a monolith biotrickling filter treating
625 high concentrations of H₂S from mimic biogas and elemental sulfur plugging
626 control using pigging, *Chemosphere.* 186 (2017) 790–797.
627 <https://doi.org/10.1016/j.chemosphere.2017.08.032>.
- 628 [17] F. Fan, B. Zhang, J. Liu, Q. Cai, W. Lin, B. Chen, Towards sulfide removal and
629 sulfate reducing bacteria inhibition: Function of biosurfactants produced by
630 indigenous isolated nitrate reducing bacteria, *Chemosphere.* 238 (2020) 124655.
631 <https://doi.org/10.1016/j.chemosphere.2019.124655>.
- 632 [18] F. Di Capua, F. Pirozzi, P.N.L. Lens, G. Esposito, Electron donors for
633 autotrophic denitrification, *Chem. Eng. J.* 362 (2019) 922–937.
634 <https://doi.org/10.1016/j.cej.2019.01.069>.
- 635 [19] D. Ucar, T. Yilmaz, F. Di Capua, G. Esposito, E. Sahinkaya, Comparison of
636 biogenic and chemical sulfur as electron donors for autotrophic denitrification in
637 sulfur-fed membrane bioreactor (SMBR), *Bioresour. Technol.* 299 (2020)
638 122574. <https://doi.org/10.1016/j.biortech.2019.122574>.
- 639 [20] D.L. Bouranis, D. Gasparatos, B. Zechmann, L.D. Bouranis, S.N.
640 Chorianopoulou, The effect of granular commercial fertilizers containing
641 elemental sulfur on wheat yield under mediterranean conditions, *Plants.* 8 (2019)

- 642 1–15. <https://doi.org/10.3390/plants8010002>.
- 643 [21] C.J.N. Buisman, B.G. Geraats, P. Ijspeert, G. Lettinga, Optimization of sulphur
644 production in a biotechnological sulphide- removing reactor, *Biotechnol.*
645 *Bioeng.* 35 (1990) 50–56. <https://doi.org/10.1002/bit.260350108>.
- 646 [22] J. Lohwacharin, A.P. Annachhatre, Biological sulfide oxidation in an airlift
647 bioreactor, *Bioresour. Technol.* 101 (2010) 2114–2120.
648 <https://doi.org/10.1016/j.biortech.2009.10.093>.
- 649 [23] B. Krishnakumar, S. Majumdar, V.B. Manilal, A. Haridas, Treatment of sulphide
650 containing wastewater with sulphur recovery in a novel reverse fluidized loop
651 reactor (RFLR), *Water Res.* 39 (2005) 639–647.
652 <https://doi.org/10.1016/j.watres.2004.11.015>.
- 653 [24] M. Fernández, M. Ramírez, J.M. Gómez, D. Cantero, Biogas biodesulfurization
654 in an anoxic biotrickling filter packed with open-pore polyurethane foam, *J.*
655 *Hazard. Mater.* 264 (2014) 529–535.
656 <https://doi.org/10.1016/j.jhazmat.2013.10.046>.
- 657 [25] M. Mora, M. Fernández, J.M. Gómez, D. Cantero, J. Lafuente, X. Gamisans, D.
658 Gabriel, Kinetic and stoichiometric characterization of anoxic sulfide oxidation
659 by SO-NR mixed cultures from anoxic biotrickling filters, *Appl. Microbiol.*
660 *Biotechnol.* 99 (2015) 77–87. <https://doi.org/10.1007/s00253-014-5688-5>.
- 661 [26] J. Brito, F. Almenglo, M. Ramírez, J.M. Gómez, D. Cantero, PID control system
662 for biogas desulfurization under anoxic conditions, *J. Chem. Technol.*
663 *Biotechnol.* 92 (2017) 2369–2375. <https://doi.org/10.1002/jctb.5243>.
- 664 [27] J. Brito, F. Almenglo, M. Ramírez, D. Cantero, Feedback and feedforward
665 control of a biotrickling filter for H₂S desulfurization with nitrite as electron
666 acceptor, *Appl. Sci.* 9 (2019) 2669. <https://doi.org/10.3390/app9132669>.
- 667 [28] K.J. Åström, T. Hägglund, PID controllers: theory, design, and tuning,
668 Instrument society of America Research Triangle Park, NC, 1995.
- 669 [29] T. Hägglund, K. Åström, Revisiting the Ziegler-Nichols Tuning Rules for PI
670 Control, *Asian J. Control.* 4 (2002) 364–380.
- 671 [30] APHA/AWWA/WEF, Standard Methods for the Examination of Water and

- 672 Wastewater, 12th ed., American Public Health Association/American Water
673 Works Association/Water Environment Federation, Washington D.C, 1999.
- 674 [31] K. Liu, J.R. Phillips, X. Sun, S. Mohammad, R.L. Huhnke, H.K. Atiyeh,
675 Investigation and modeling of gas-liquid mass transfer in a sparged and non-
676 sparged continuous stirred tank reactor with potential application in syngas
677 fermentation, *Fermentation*. 5 (2019).
678 <https://doi.org/doi:10.3390/fermentation5030075>.
- 679 [32] J.E. Duddridge, C.A. Kent, J.F. Laws, Effect of surface shear stress on the
680 attachment of *Pseudomonas fluorescens* to stainless steel under defined flow
681 conditions, *Biotechnol. Bioeng.* 24 (1982) 153–164.
682 <https://doi.org/10.1002/bit.260240113>.
- 683 [33] J.C. Merchuk, Shear effects on suspended cells, in: *Bioreact. Syst. Eff.*, Springer
684 Berlin Heidelberg, Berlin, Heidelberg, 1991: pp. 65–95.
685 <https://doi.org/10.1007/Bfb0000748>.
- 686 [34] P. Jonczyk, M. Takenberg, S. Hartwig, S. Beutel, R.G. Berger, T. Scheper,
687 Cultivation of shear stress sensitive microorganisms in disposable bag reactor
688 systems, *J. Biotechnol.* 167 (2013) 370–376.
689 <https://doi.org/10.1016/j.jbiotec.2013.07.018>.
- 690 [35] D. Gómez-Ríos, S. Junne, P. Neubauer, S. Ochoa, R. Ríos-Esteba, H. Ramírez-
691 Malule, Characterization of the metabolic response of *Streptomyces clavuligerus*
692 to shear stress in stirred tanks and single-use 2D rocking motion bioreactors for
693 clavulanic acid production, *Antibiotics*. 8 (2019) 1–16.
694 <https://doi.org/10.3390/antibiotics8040168>.
- 695 [36] W. Logroño, D. Popp, S. Kleinstüber, H. Sträuber, H. Harms, M. Nikolausz,
696 Microbial resource management for ex situ biomethanation of hydrogen at
697 alkaline pH, *Microorganisms*. 8 (2020) 614.
698 <https://doi.org/10.3390/microorganisms8040614>.
- 699 [37] D. Pokorna, J. Zabranska, Sulfur-oxidizing bacteria in environmental technology,
700 *Biotechnol. Adv.* 33 (2015) 1246–1259.
701 <https://doi.org/10.1016/j.biotechadv.2015.02.007>.
- 702 [38] J. Cai, P. Zheng, Q. Mahmood, Effect of sulfide to nitrate ratios on the

- 703 simultaneous anaerobic sulfide and nitrate removal, *Bioresour. Technol.* 99
704 (2008) 5520–5527. <https://doi.org/10.1016/j.biortech.2007.10.053>.
- 705 [39] L.R. López, J. Brito, M. Mora, F. Almenglo, J.A. Baeza, M. Ramírez, J.
706 Lafuente, D. Cantero, D. Gabriel, Feedforward control application in aerobic and
707 anoxic biotrickling filters for H₂S removal from biogas, *J. Chem. Technol.*
708 *Biotechnol.* 93 (2018) 2307–2315. <https://doi.org/10.1002/jctb.5575>.
- 709 [40] X. Li, X. Jiang, Q. Zhou, W. Jiang, Effect of S/N ratio on the removal of
710 hydrogen sulfide from biogas in anoxic bioreactors, *Appl. Biochem. Biotechnol.*
711 180 (2016) 930–944. <https://doi.org/10.1007/s12010-016-2143-3>.
- 712 [41] P.I. Cano, J. Brito, F. Almenglo, M. Ramírez, J.M. Gómez, D. Cantero, Influence
713 of trickling liquid velocity, low molar ratio of nitrogen/sulfur and gas-liquid flow
714 pattern in anoxic biotrickling filters for biogas desulfurization, *Biochem. Eng. J.*
715 148 (2019) 205–213. <https://doi.org/10.1016/j.bej.2019.05.008>.
- 716 [42] P. Dolejs, L. Paclík, J. Maca, D. Pokorna, J. Zabranska, J. Bartacek, Effect of
717 S/N ratio on sulfide removal by autotrophic denitrification, *Appl. Microbiol.*
718 *Biotechnol.* 99 (2015) 2383–2392. <https://doi.org/10.1007/s00253-014-6140-6>.
- 719 [43] N.J.R. Kraakman, J. Rocha-Rios, M.C.M. Van Loosdrecht, Review of mass
720 transfer aspects for biological gas treatment, *Appl. Microbiol. Biotechnol.* 91
721 (2011) 873–886. <https://doi.org/10.1007/s00253-011-3365-5>.
- 722 [44] Q. Mahmood, P. Zheng, J. Cai, D. Wu, B. Hu, J. Li, Anoxic sulfide biooxidation
723 using nitrite as electron acceptor, *J. Hazard. Mater.* 147 (2007) 249–256.
724 <https://doi.org/10.1016/j.jhazmat.2007.01.002>.
- 725 [45] E. Can-Dogan, M. Turker, L. Dagan, A. Arslan, Sulfide removal from
726 industrial wastewaters by lithotrophic denitrification using nitrate as an electron
727 acceptor, *Water Sci. Technol.* 62 (2010) 2286–2293.
728 <https://doi.org/10.2166/wst.2010.545>.
- 729 [46] C. Fajardo, A. Mosquera-Corral, J.L. Campos, R. Méndez, Autotrophic
730 denitrification with sulphide in a sequencing batch reactor, *J. Environ. Manage.*
731 113 (2012) 552–556. <https://doi.org/10.1016/j.jenvman.2012.03.018>.
- 732 [47] R. Kleerebezem, R. Mendez, Autotrophic denitrification for combined hydrogen

- 733 sulfide removal from biogas and post-denitrification., *Water Sci. Technol.* 45
734 (2002) 349–356. <https://doi.org/10.2166/wst.2002.0368>.
- 735 [48] I. Manconi, A. Carucci, P. Lens, Combined removal of sulfur compounds and
736 nitrate by autotrophic denitrification in bioaugmented activated sludge system,
737 *Biotechnol. Bioeng.* 98 (2007) 551–560. <https://doi.org/10.1002/bit.21383>.
- 738 [49] A. Roosta, A. Jahanmiri, D. Mowla, A. Niazi, H. Sotoodeh, Optimization of
739 biological sulfide removal in a CSTR bioreactor, *Bioprocess Biosyst. Eng.* 35
740 (2012) 1005–1010. <https://doi.org/10.1007/s00449-012-0685-5>.
- 741 [50] A.M. Montebello, M. Mora, L.R. López, T. Bezerra, X. Gamisans, J. Lafuente,
742 M. Baeza, D. Gabriel, Aerobic desulfurization of biogas by acidic biotrickling
743 filtration in a randomly packed reactor, *J. Hazard. Mater.* 280 (2014) 200–208.
744 <https://doi.org/10.1016/j.jhazmat.2014.07.075>.
- 745 [51] M.A.M. Zytoon, A.A. AlZahrani, M.H. Noweir, F.A. El-Marakby, Bioconversion
746 of high concentrations of hydrogen sulfide to elemental sulfur in airlift
747 bioreactor, *Sci. World J.* 2014 (2014) 675673.
748 <https://doi.org/10.1155/2014/675673>.
- 749 [52] F. Almenglo, T. Bezerra, J. Lafuente, D. Gabriel, M. Ramírez, D. Cantero, Effect
750 of gas-liquid flow pattern and microbial diversity analysis of a pilot-scale
751 biotrickling filter for anoxic biogas desulfurization, *Chemosphere.* 157 (2016)
752 215–223. <https://doi.org/10.1016/j.chemosphere.2016.05.016>.
- 753 [53] X. Jiang, J. Wu, Z. Jin, S. Yang, L. Shen, Enhancing the removal of H₂S from
754 biogas through refluxing of outlet gas in biological bubble-column, *Bioresour.*
755 *Technol.* 299 (2020) 122621. <https://doi.org/10.1016/j.biortech.2019.122621>.
- 756 [54] C. Jing, Z. Ping, Q. Mahmood, Influence of various nitrogenous electron
757 acceptors on the anaerobic sulfide oxidation, *Bioresour. Technol.* 101 (2010)
758 2931–2937. <https://doi.org/10.1016/j.biortech.2009.11.047>.
- 759 [55] M. Fernández, M. Ramírez, R.M. Pérez, J.M. Gómez, D. Cantero, Hydrogen
760 sulphide removal from biogas by an anoxic biotrickling filter packed with Pall
761 rings, *Chem. Eng. J.* 225 (2013) 456–463.
762 <https://doi.org/10.1016/j.cej.2013.04.020>.

- 763 [56] Y. Zeng, L. Xiao, X. Zhang, J. Zhou, G. Ji, S. Schroeder, G. Liu, Z. Yan, Biogas
764 desulfurization under anoxic conditions using synthetic wastewater and biogas
765 slurry, *Int. Biodeterior. Biodegrad.* 133 (2018) 247–255.
766 <https://doi.org/10.1016/j.ibiod.2018.05.012>.
- 767 [57] L.R. López, T. Bezerra, M. Mora, J. Lafuente, D. Gabriel, Influence of trickling
768 liquid velocity and flow pattern in the improvement of oxygen transport in
769 aerobic biotrickling filters for biogas desulfurization, *J. Chem. Technol.*
770 *Biotechnol.* 91 (2016) 1031–1039. <https://doi.org/10.1002/jctb.4676>.
- 771 [58] P.G. Aguilera, F.J. Gutiérrez Ortiz, Techno-economic assessment of biogas plant
772 upgrading by adsorption of hydrogen sulfide on treated sewage–sludge, *Energy*
773 *Convers. Manag.* 126 (2016) 411–420.
774 <https://doi.org/10.1016/j.enconman.2016.08.005>.
- 775
- 776
- 777
- 778
- 779
- 780
- 781
- 782
- 783

Biological desulfurization of biogas has been extensively studied using biotrickling filters (BTFs). However, the accumulation of elemental sulfur (S^0) on the packing material limits the use of this technology. To overcome this issue, the use of a continuous stirred tank bioreactor (CSTBR) under anoxic conditions for biogas desulfurization and S^0 production is proposed in the present study. The effect of the main parameters (stirring speed, N/S molar ratio, hydraulic residence time (HRT) and gas residence time (GRT)) on the bioreactor performance was studied. Under an inlet load (IL) of $100 \text{ g S-H}_2\text{S m}^{-3} \text{ h}^{-1}$ and a GRT of 119 s, the CSTBR optimal operating conditions were 60 rpm, N/S molar ratio of 1.1 and a HRT of 42 h, in which a removal efficiency (RE) and S^0 production of $98.6 \pm 0.4\%$ and 88% were obtained, respectively. Under a GRT of 41s and an IL of $232 \text{ g S-H}_2\text{S m}^{-3} \text{ h}^{-1}$ the maximum elimination capacity (EC) of $166.0 \pm 7.2 \text{ g S-H}_2\text{S m}^{-3} \text{ h}^{-1}$ (RE = $71.7 \pm 3.1\%$) was obtained. A proportional-integral feedback control strategy was successfully applied to the bioreactor operated under a stepped variable IL.

José Joaquín González-Cortés: Investigation, Formal analysis, Writing- Original draft preparation. **Sandra Torres-Herrera:** Investigation. **Fernando Almenglo:** Conceptualization, Methodology, Supervision. **Martín Ramírez:** Conceptualization, Methodology, Supervision, Project administration, Funding acquisition, Writing- Reviewing and Editing. **Domingo Cantero:** Conceptualization, Project administration, Funding acquisition, Writing- Reviewing and Editing.

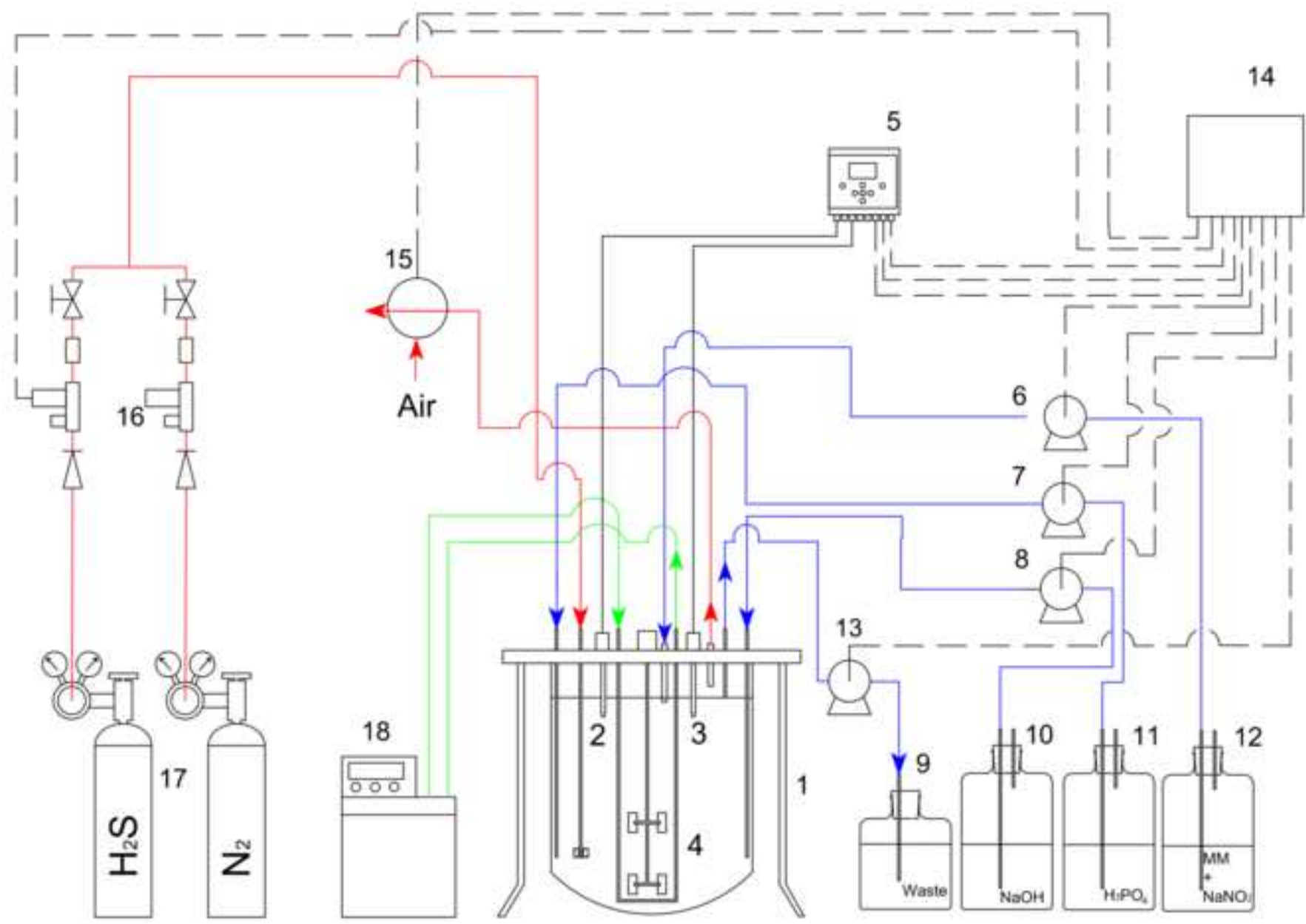
Novelty Statement

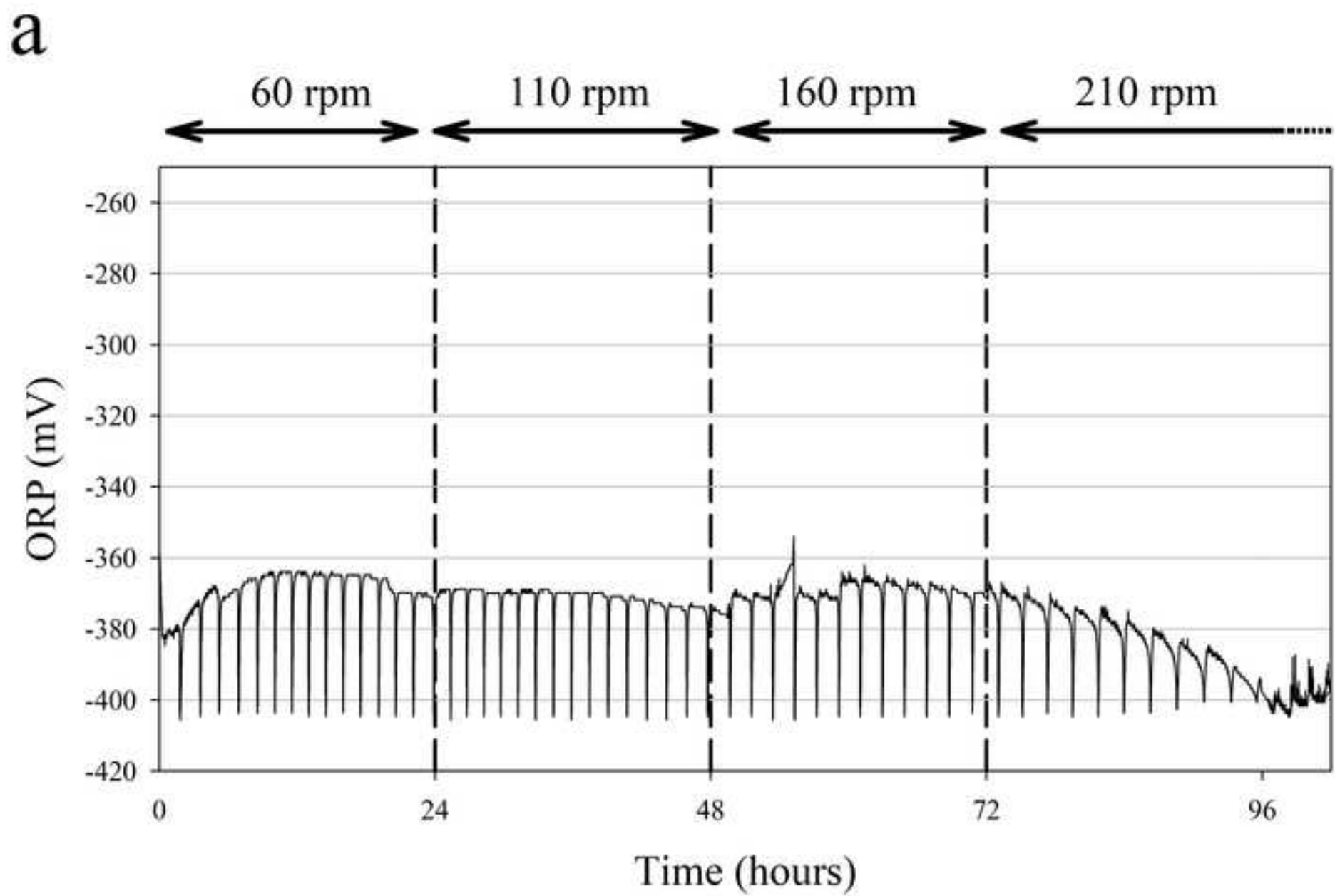
An efficient bioprocess (anoxic desulfurization from biogas) has been successfully optimized in a CSTBR for the first time, achieving similar elimination capacities than the widely-studied biotrickling filters. Additional novel features such as the SO-NR biomass sensitiveness to shear-stress forces or the dilution study are described.

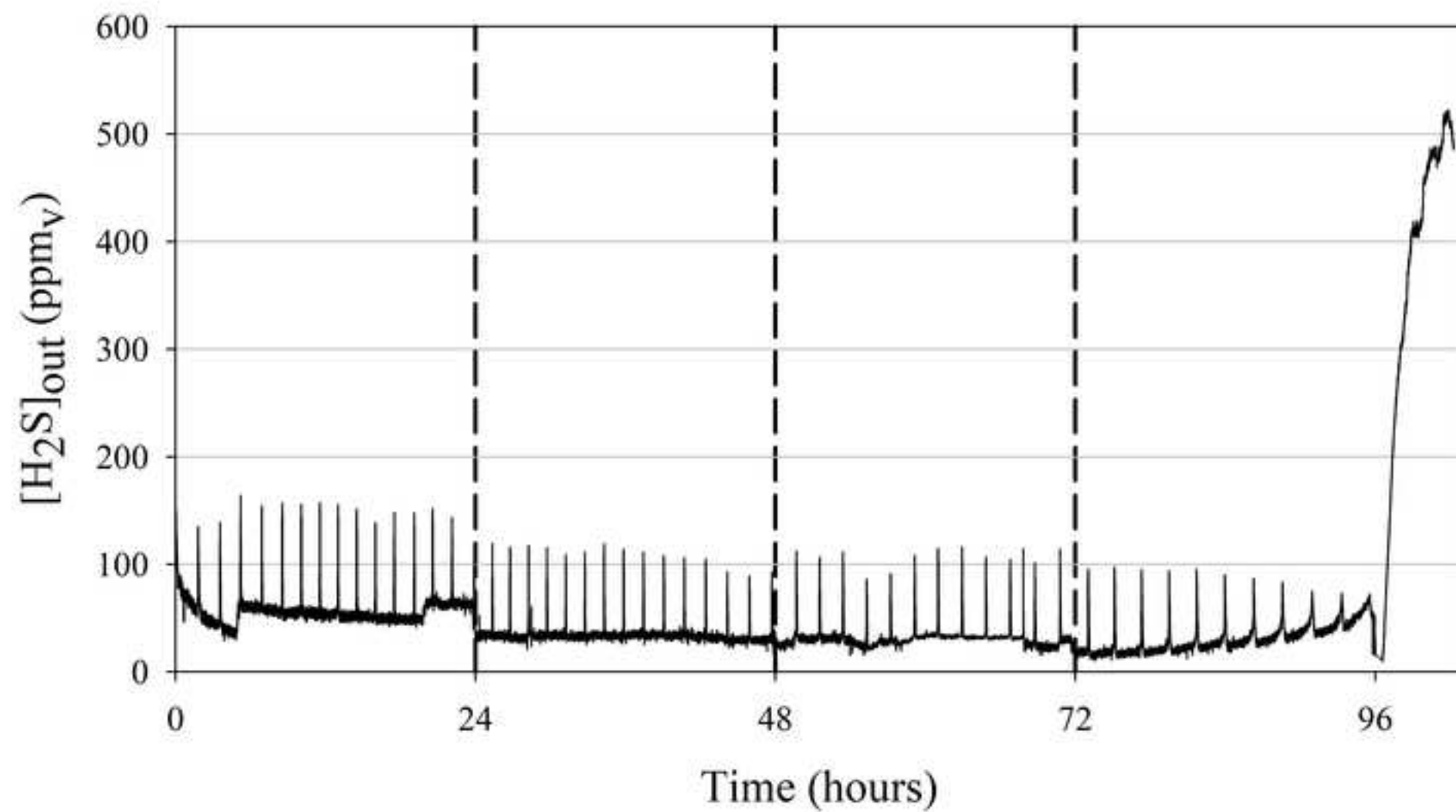
Hydrogen sulfide (H₂S), a ubiquitous compound strongly toxic to the environment and the human-health, stands as the main hazardous material removed in the study. Its conversion to recoverable and re-usable elemental sulfur at the same time as nitrite (another toxic compound) is reduced to harmless N₂ is proposed in the present work.

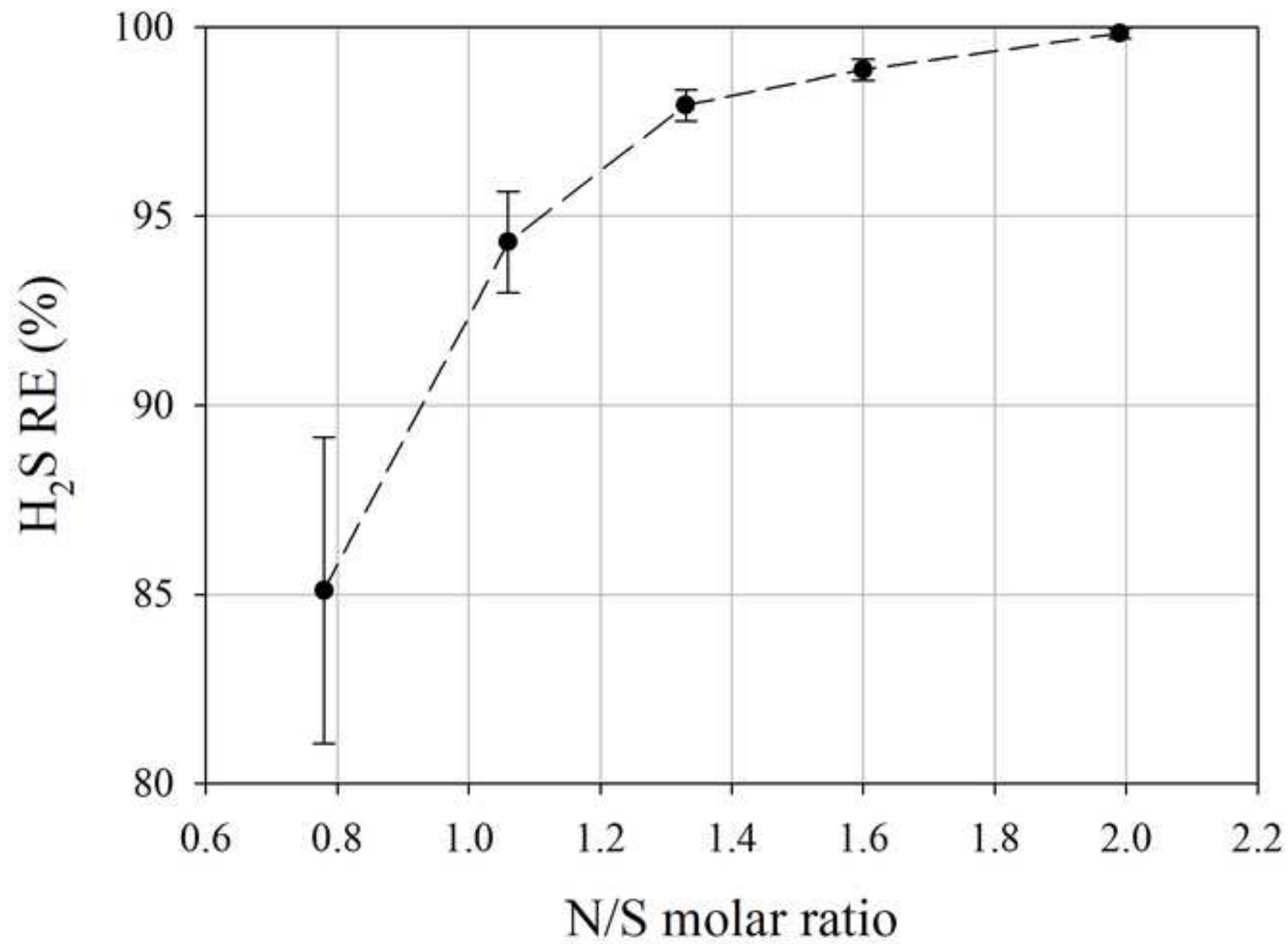
Table 1. Operational conditions of the different experiments carried out.

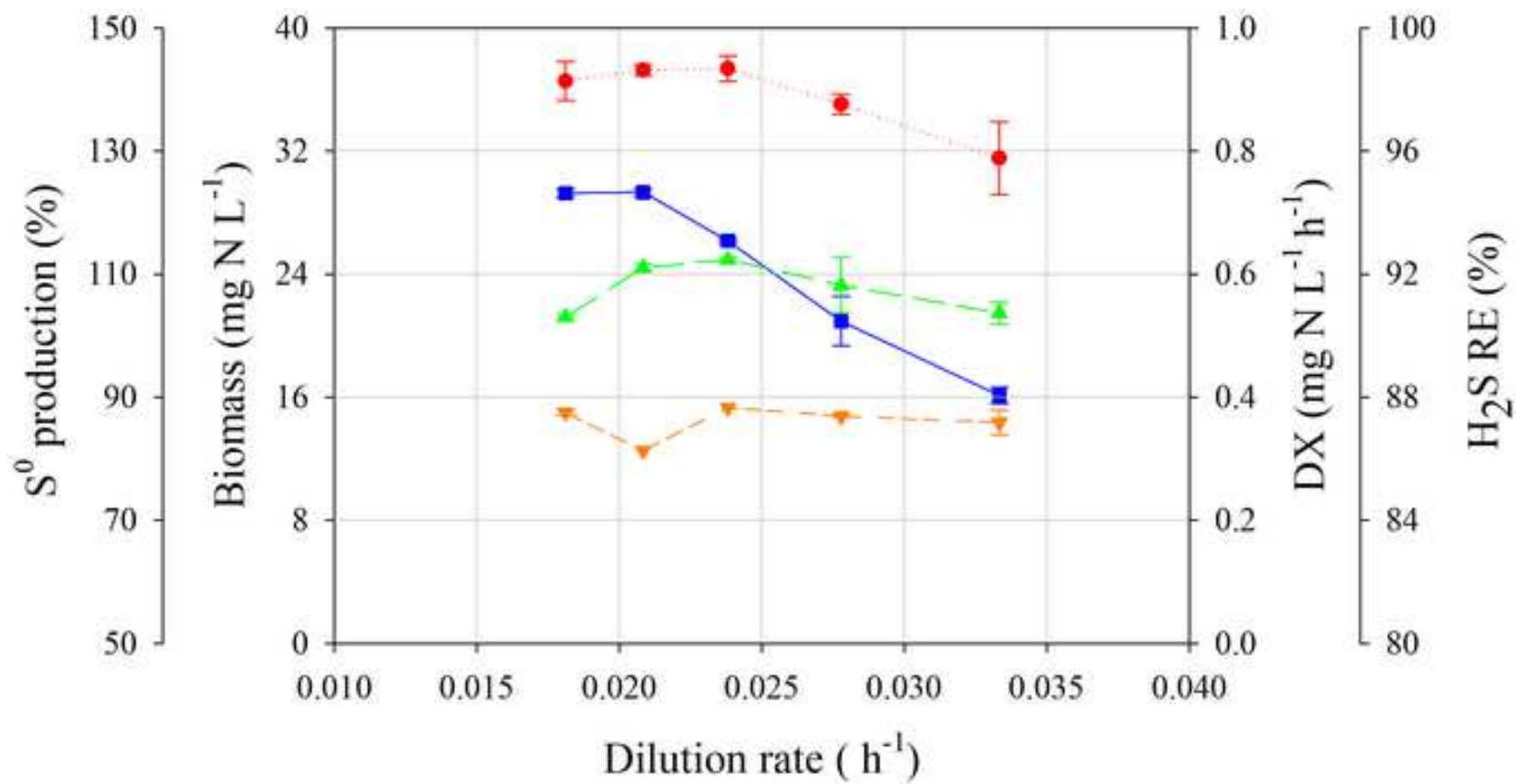
Exp.	IL (gS-H ₂ S m ⁻³ h ⁻¹)	HRT(h)	GRT(s)	N/S molar ratio (mol:mol ⁻¹)	Stirring speed (rpm)	[H ₂ S] _{in} (ppmv)	Studied Variable	Days
1	70	-	139	Variable	60 110 160 210	1800	Stirring speed	7
2	100	66 47 36 30	119	1.99 1.6 1.33 1.06 0.78	60	2500	N/S molar ratio	1
3	100	55 48 42 36 30	119	1.1	60	2500	HRT	40
4.1	100	42	119 104 89 73 57 41	1.1	60	2500 2171 1841 1512 1182 853	GRT (constant IL)	1
4.2	79 90 106 129 165 232	59 51 43 36 28 20	119 104 89 73 57 41	1.1	60	2000	GRT (constant [H ₂ S] _{in})	1
5	139-73	40-21.5	119	1.6-0.9	60	3500-1850	Stepwise changes in IL	3

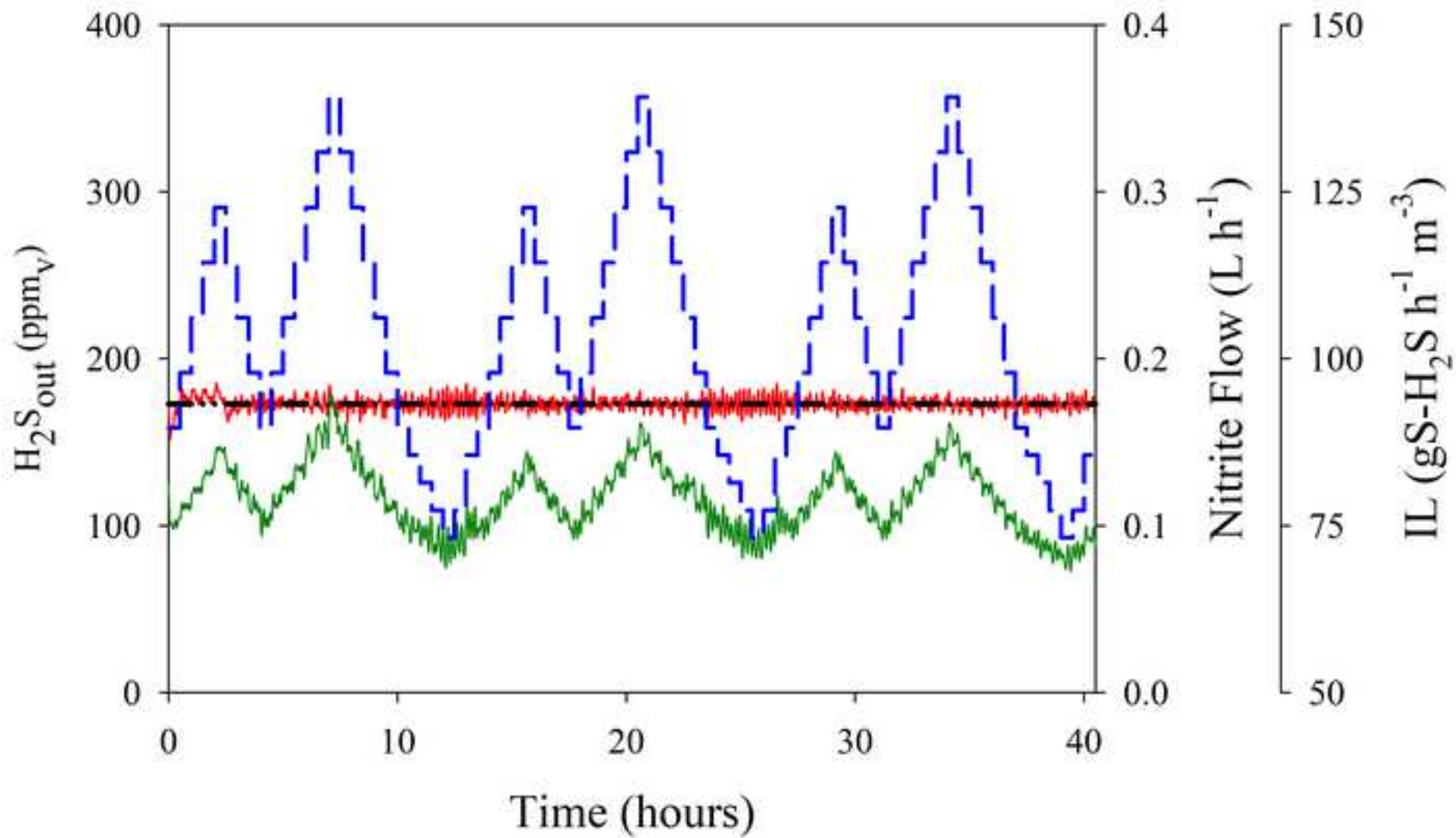




b







1 **Anoxic biogas biodesulfurization promoting elemental sulfur production in a**
2 **Continuous Stirred Tank Bioreactor**

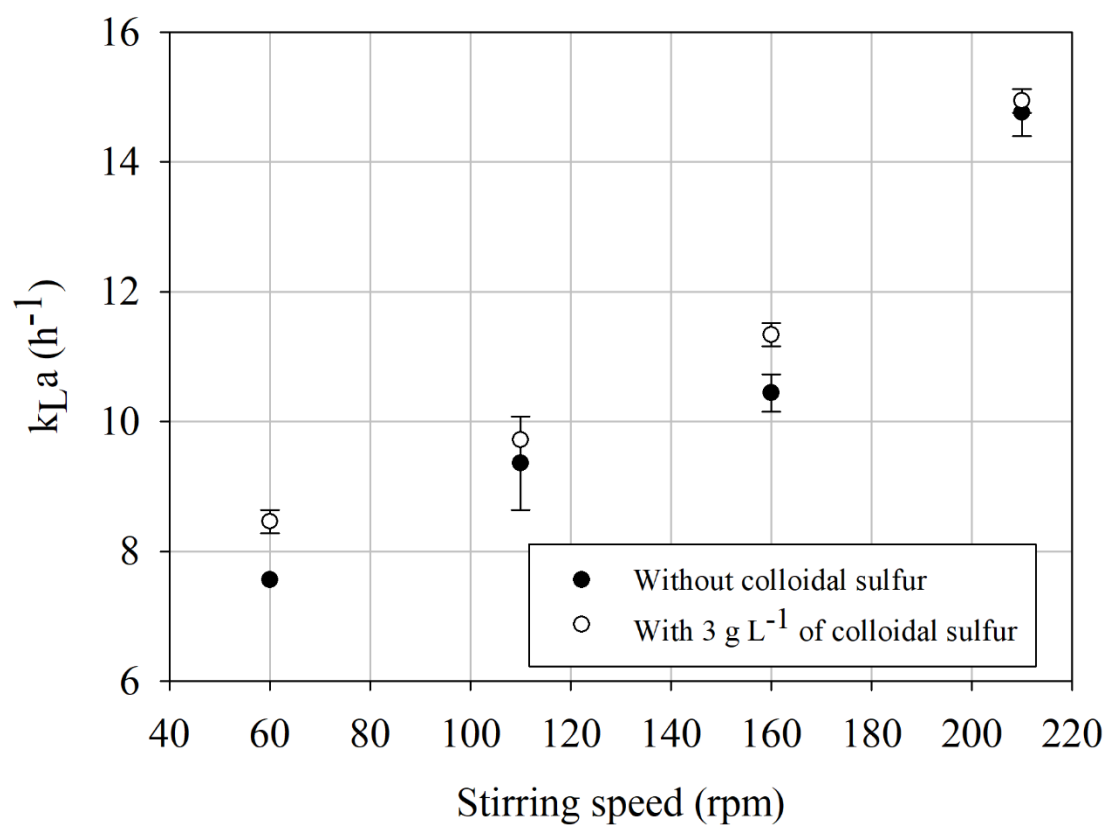
3

4 José Joaquín González-Cortés, Sandra Torres-Herrera, Fernando Almenglo, Martín Ramírez,
5 Domingo Cantero.

6 ***SUPPLEMENTARY MATERIAL***

7

8 **Supplementary figures and tables.**



9

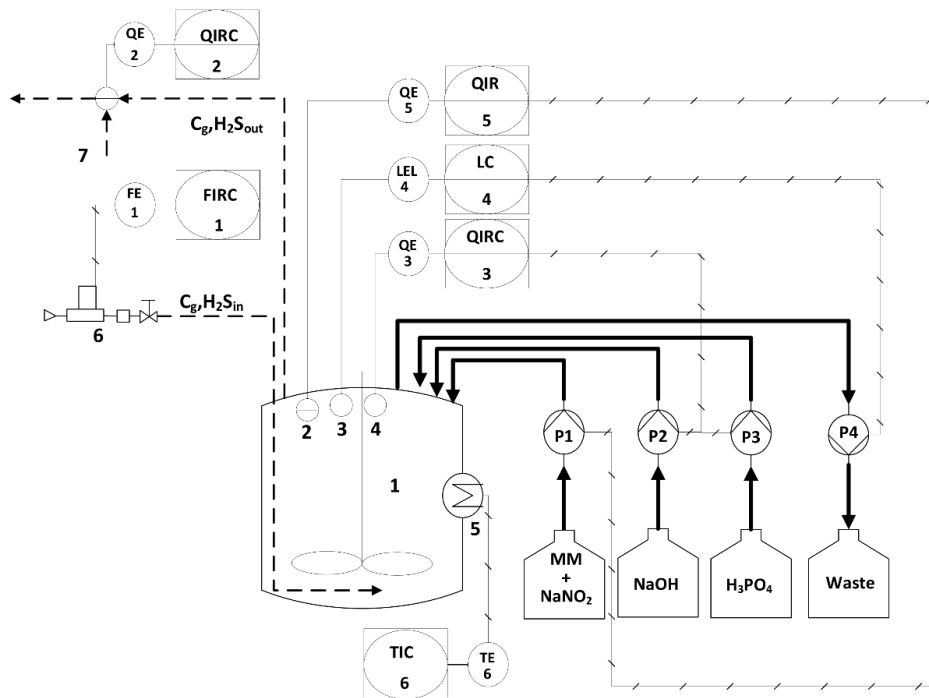
10 **Fig. S1** – k_{La} determination at different stirring speeds under a GRT of 139 s.

11

12

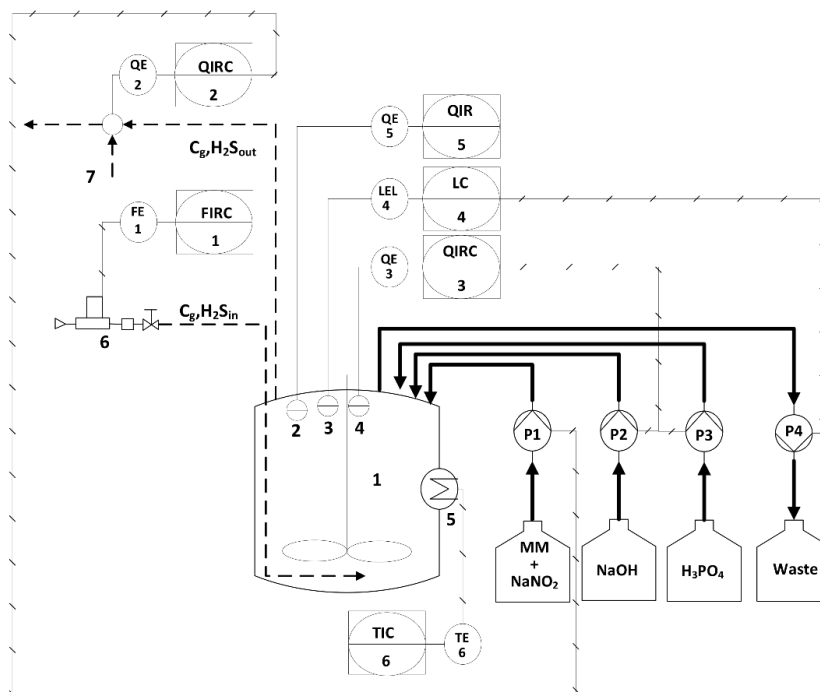
13

14



15

16 **Fig. S2** – Schematic of the control system. 1. CSTBR; 2. ORP sensor; 3. Level sensor; 4. pH sensor; 5.
 17 Heat exchanger; 6. Mass flow controller. 7. H₂S sensor with a dilution system.
 18 FIRC, flow rate indicator recording controller; QIRC, quantity indicator recording controller,
 19 QIR, quantity indicator recording; LC, level control; TIC, temperature indicator controller. Control loops:
 20 1 (gas flow rate), 2 (H₂S concentration), 3 (pH), 4 (level), 5 (nitrite flow rate) and 6 (temperature).



21

22 **Fig. S3** – Schematic of the control system. 1. CSTBR; 2. ORP sensor; 3. Level sensor; 4. pH sensor; 5.
 23 Heat exchanger; 6. Mass flow controller. 7. H₂S sensor with a dilution system.
 24 FIRC, flow rate indicator recording controller; QIRC, quantity indicator recording controller,
 25 QIR, quantity indicator recording; LC, level control; TIC, temperature indicator controller. Control loops:
 26 1 (gas flow rate), 2 (nitrite flow rate), 3 (pH), 4 (level), 5 (ORP) and 6 (temperature).

27



28

29

30 **Fig. S4** – Picture of the stirred tank bioreactor accumulating elemental sulfur as the main oxidation product.

31

32

33 **Biomass growth calculation**

34

35
$$Y_{X/S^{2-}} \left(\frac{g \text{ VSS}}{g \text{ S}^{2-}} \right) = \frac{\text{Dilution (h}^{-1}) \times \text{Biomass (g VSS m}^{-3}) \times 100}{IL \text{ (g S-H}_2\text{S m}^{-3} \text{ h}^{-1}) \times RE (\%)}$$
 (Eq. S1)

36

37

38